ORGANOMETALLICS

ARTICLE

pubs.acs.org/Organometallics

Systematic Investigation of Ligand Substitution Effects in Cyclophane-Based Nickel(II) and Palladium(II) Olefin Polymerization Catalysts[1]

Chris S. Popeney, Chris M. Levins, and Zhibin Guan*

Department of Chemistry, University of California, 1102 Natural Sciences 2, Irvine, California 92697, United States

Supporting Information

ABSTRACT: The synthesis of Ni(II) and Pd(II) cyclophane-based α-diimine olefin polymerization catalysts bearing a range of electron-donating or -withdrawing groups is described. Substituent effects were confirmed by measurement of CO infrared stretching frequencies in Pd(II) carbonyl complexes. Polymerizations with ethylene were investigated in detail involving determination of catalyst productivity and thermal stability, especially at elevated temperature, as well as analysis of polymer molecular weight and microstructure. The Ni(II) catalysts, formed by *in situ* treatment of tetraarylborate salts of $[Ni(diimine)(acac)]^+$ with triisobutylaluminum, exhibited little variation in productivity or thermal stability across the substitution series, but the resulting polymers showed an increase in both molecular weight and branching density for catalysts with increasingly electron-withdrawing character. The chloride-substituted Pd(II) analogue, however, was notable in its markedly higher productivity and thermal stability at elevated temperature compared to the other substituted Pd(II) cyclophane catalysts, which otherwise showed little variation, like the Ni(II) catalysts. Unlike the previously studied acyclic Pd(II) α-diimine catalysts, a strong tendency toward higher molecular weight polymer with more electron-deficient catalysts was noted. An alternative dissociative chain transfer mechanism is proposed to account for this difference, as well as the generally lower than expected molecular weight of the cyclophane catalysts. As a further explanation for the unusual behavior of these catalysts, NMR evidence of a stabilizing ligand−metal H-agostic interaction in the case of the Pd(II) system is also reported.

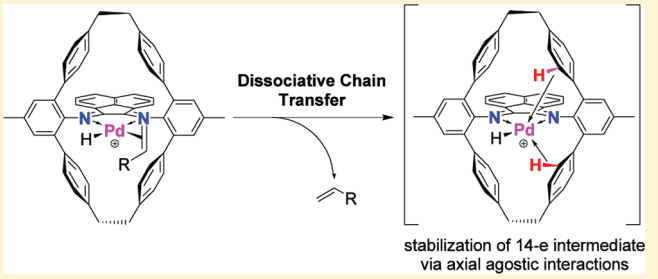

INTRODUCTION

A key development in late transition metal olefin polymerization catalysis was the discovery of the requirement of ligand steric bulk to achieve high polymerization activity and molecular weight.[2−4] The bis-aryl-substituted α-diimine ligand achieves this goal through the suppression of associative chain transfer by sterically blocking access of the monomer to the axial metal coordination sites. In addition, the functional group tolerance of the Pd(II) α-diimine system,[5,6] and its ability to incorporate polar comonomers,[5,7,8] has found synthetic utility in the preparation of unique functional polymer architectures. Despite the promise of the Pd(II) and Ni(II) α-diimine systems, however, they have several limitations. Both systems have relatively low thermal stability and are prone to significant chain transfer at elevated temperatures, affording low molecular weight polymer in low yields.[5,9,10] These features are undesirable for practical polymerization processes, many of which are optimized for efficient operation only at high temperatures.[11]

To address some of the limitations of the standard acyclic α-diimine complexes, our group has developed a cyclophane-based α-diimine ligand (Me-Cyc, ligand **1c** in Chart 1) for late transition metal olefin polymerization catalysis.[12−14] The cyclophane ligand was envisioned to offer even greater protection from axial monomer approach because of its inherently rigid nature. Cyclophanes are macrocyclic compounds composed of aromatic and aliphatic moieties and have found interest in conformational,[15] host−guest,[16] and supramolecular studies.[17] The structures of cyclophanes are attractive for use as ligands in olefin polymerization since the ligand can appropriately surround the metal, offering potential improvement in protection against chain-termination processes. Furthermore, it was anticipated that the closed cyclic structure of the cyclophane ligand, through conformational rigidity, would inhibit deactivation processes such as C−H activation,[10] increase polymer molecular weight by limiting associative chain transfer, and lead to a more robust catalyst.

As an example of the reduction in associative chain transfer and the increase in catalyst stability, Ni(II) cyclophane-based catalysts were shown to produce polyethylene at very high activity with high molecular weight at temperatures up to 90 °C.[12] Furthermore, the Ni(II) cyclophane-based catalysts exhibit living polymerization behavior for α-olefin polymerizations at temperatures up to 75 °C.[14] In addition to the desired

Received: March 1, 2011
Published: March 30, 2011

Chart 1. Substituted Cyclophane-Based α-Diimine Ligands 1a−e, Ni(II) Complexes 2a−e, and Pd(II) Complexes 3a−e

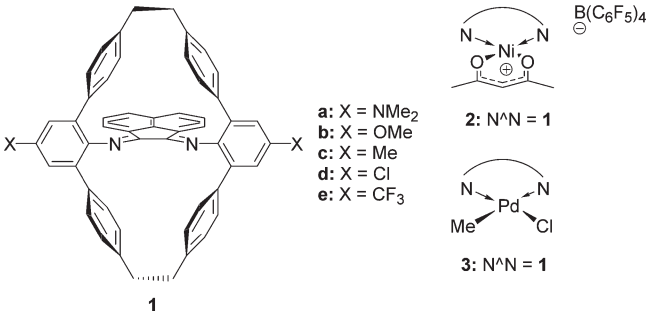

effects on chain transfer rate and stability, other polymerization properties were found to be significantly different than those observed for catalysts bearing the standard acyclic α-diimine ligands. For example, the branching density of polypropylene was significantly decreased with the Ni(II) cyclophane catalyst compared to the acyclic catalyst.[14] The cyclophane Pd(II) catalyst incorporated substantially higher amounts of polar olefin comonomers than the acyclic analogue,[18] an effect subsequently found to result from the inhibition of olefin exchange processes due to ligand steric bulk in the axial positions.[19]

Our previous studies have shown that the introduction of substituents to the *para*-aryl ligand position of acyclic Pd(II) α-diimine catalysts led to significant perturbation of catalytic properties.[20] With electron-donating groups installed, the catalysts afforded polyethylene of less heavily branched topology. In addition, dramatic changes in the tolerance of the catalysts to polar monomers were also observed. Electron-rich catalysts were able to incorporate larger amounts of acrylates in higher activities than the catalysts bearing electron-withdrawing groups. In more recent investigations, the presence of electron-donating groups imparted higher thermal stability and longevity on the catalysts and gave rise to polymers of higher molecular weight because of the reduction of associative chain transfer.[21] On the basis of these findings, we have carried out a systematic investigation on the effect of *para*-substitution in Ni(II) and Pd(II) cyclophane-based α-diimine catalysts bearing substituted ligands **1a**−**e** in order to improve upon their polymerization capabilities. Details regarding the catalytic activity and thermal stability of the Ni(II)- and Pd(II)-substituted cyclophane-based catalysts **2a**−**e** and **3a**−**e** (Chart 1), along with analysis of the polymer molecular weight and microstructure, will be presented in this paper. The results of these experiments will be combined with those of the previous studies to further reveal some unusual mechanistic features of the cyclophane catalytic system.

RESULTS

Synthesis of Substituted Cyclophane-Based α-Diimine Ligands. The synthesis of the substituted cyclophane-based ligands (X-Cyc) was performed in a manner similar to the published synthetic route for the parent member of the series: methyl-substituted ligand **1c**.[12,13] The key steps were a cross-coupling reaction to provide a divinyl *meta*-terphenyl aniline and ring-closing olefin metathesis to convert an open terphenyl-based diimine into the cyclophane structure. Due to the synthetic requirements of the study, a more efficient one-step method in the preparation of substituted terphenyl anilines directly from simple aniline precursors was developed.

Dimethylamino-substituted aniline **4a** was synthesized via an efficient three-step route (Scheme 1): oxidation of 2,6-dibromo-4-fluoroaniline **5** to the nitro analogue **6**, amination to afford **7** by fluoride displacement, and reduction by tin(II) chloride to give aniline **4a**. Methoxy-substituted dibromoaniline **4b** was prepared following the literature procedure.[22] The chloro- and trifluoromethyl-substituted dibromoanilines **4d** and **4e** were commercially available. Although a logical addition to the series, a nitro-substituted analogue was not prepared because of the low stability of the nitro-substituted acyclic Pd(II) catalysts as noted from our previous studies.[20,21]

Moderate yields of terphenyl anilines **8b**,**c**,**d** were afforded by the Negishi reaction using the $Pd_2(dba)_3$/S-Phos catalyst system reported by Buchwald and co-workers[23] (S-Phos = 2-dicyclohexylphosphino-2′,6′-dimethoxybiphenyl) and 4-vinylphenylzinc chloride. Both NMe_2-substituted aniline **8a** and CF_3-substituted aniline **8e**, however, were prepared inefficiently by this method, although the Suzuki protocol using 4-vinylphenylboronic acid **9** and the $Pd(OAc)_2$/S-Phos system afforded these targets and chloro-substituted **8d** in good yield. The Suzuki reaction is likely to be the more efficient route in general but was not attempted on **8b**,**c** since an adequate amount of material was already synthesized by the Negishi route. In any case, only minimal side product formation, such as Heck reaction products, was observed, rendering this approach a convenient method for the preparation of multigram quantities of divinyl *m*-terphenyl anilines in one step (Scheme 2).

In the construction of the cyclophane α-diimine ligands from terphenyl anilines, modifications of the reported route were sometimes necessary due to the effects of specific substitution (Scheme 3).[12] This was especially true for the trifluoromethyl-substituted analogues. The condensation of electron-poor CF_3-substituted aniline **8e**, for example, required longer reaction duration at lower temperature to afford the corresponding diimine **10e** with minimal side reactions. Precautions were taken to minimize the hydrolysis of diimine **10e** during purification, likely owing to its higher electrophilicity. In addition, ring-closing metathesis to give the cyclic diimine **11e** required more forcing conditions than usual to reach high conversion. The methoxy-substituted analogues exhibited reduced solubility compared to the others, allowing for simple purification of diimine **10b** but complicating the subsequent hydrogenation of **11b** to the methoxy-substituted ligand (OMe-Cyc, **1b**). Hydrogenation could not be reproducibly performed on any of the ligands without varying amounts of over-reduction, possibly due to the presence of trace acid in the Pd/C catalyst. The addition of triethylamine circumvented this problem to afford ligands **1a**−**e** cleanly in good yield.

Ethylene Polymerization with Substituted Cyclophane-Based Ni(II) Catalysts. Nickel dihalide complexes of diimine ligands are typical catalytic precursors for use in olefin polymerizations.[3] Preparation of nickel dibromo complexes of the substituted cyclophane catalysts was attempted by reacting the ligands with Ni(DME)Br_2 (DME = 1,2-dimethoxyethane), but only partial conversion was achieved in the case of the electron-poor chloro- and trifluoromethyl-substituted ligands. Alternatively, the preparation of the cationic acetylacetonato (acac) complexes $[Ni(diimine)(acac)]^+$,[24] successful in the recent preparation of other Ni(II) complexes of bulky diimine ligands,[25] by reaction of the cyclophane ligands **1a**−**e** with trityl tetrakis(pentafluorophenyl)borate and Ni(acac)$_2$ cleanly gave

Scheme 1. Synthesis of Dimethylamino-Substituted Aniline 4a

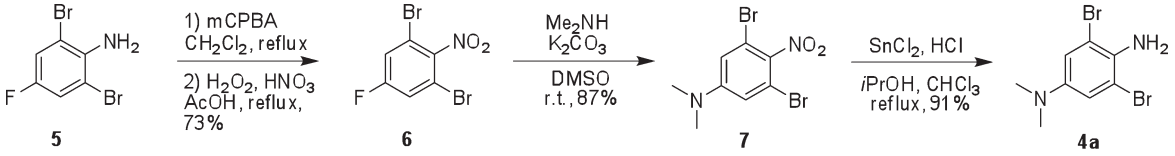

Scheme 2. Synthesis of Terphenyl Anilines 8a−e from Dibromoanilines 4a−e by Negishi or Suzuki Methods[a]

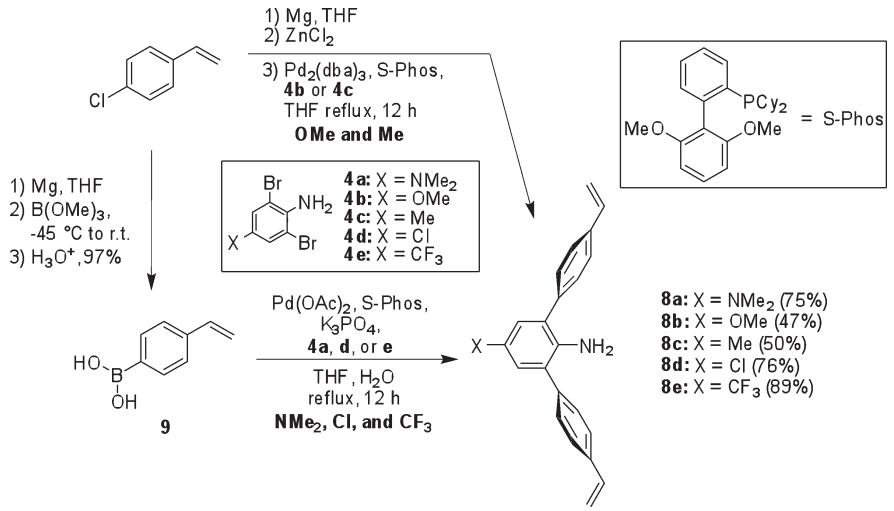

[a] Yields shown are from the Suzuki reaction except for **8b,c**.

the corresponding [Ni(diimine)(acac)]$B(C_6F_5)_4$ salts **2a**−**e** in high yields (Scheme 4). In addition to their facile formation, complexes **2a**−**e** are all diamagnetic because of their square-planar geometry and were thus characterizable by NMR. Due to the inability to obtain methoxy-substituted ligand **1b** pure (because of its low solubility, see above), the corresponding complex **2b** was accompanied by a small amount of inseparable impurities, mainly the corresponding unhydrogenated complex. For comparison to the standard acyclic archetype, acyclic analogue **12** was prepared as a control. Similarly, the dibromo Ni(Me-Cyc)Br_2 complex **13** was also studied to allow the comparison in activation ability of that more familiar system to the Ni(acac) system employed in this study.

Polymerizations with Me-Cyc complex **2c** were screened with a few organoaluminum activators at 35 and 80 °C at an Al/Ni ratio of 1500 (Figure S1, Supporting Information). At 35 °C, modified methylaluminoxane (MMAO) gave the highest polymerization productivity (measured as polymer yield), while trimethylaluminum (TMA) was slightly less active and triisobutylaluminum (TIBA) was largely ineffective. Activation efficiencies at 80 °C were reversed so that activation with TIBA became the most efficient, while activation by both MMAO and TMA gave lower productivity. Because high-temperature polymerizations were of primary interest in this study, TIBA was chosen as the activator.

Polymerizations of 10 min duration with complexes **2a**−**e** were examined at temperatures ranging from 60 to 115 °C (Table 1). Catalytic productivities were highest at 60 °C for activation by TIBA, then decreased steadily at higher temperatures because of catalyst decomposition. For comparison, the polymerizations with acyclic complex **12** (entries 1 and 2) and Ni(Me-Cyc)Br_2 **13** (entry 14, MMAO-activated) are also shown. The low thermal stability of the acyclic catalyst **12** was especially evident by the 4-fold polymer productivity decrease from 55 to 70 °C (entries 1 and 2). In contrast, the cyclophane catalysts **2a**−**e** had similar activity at 115 °C to the acyclic catalyst at 70 °C, demonstrating the thermal stability provided by the cyclophane ligand. The polymerization productivities of the **13**/MMAO and **2c**/TIBA systems were comparable at 80 °C, indicating that both activation methods likely lead to catalytic species of the same reactivity. The productivity was adjusted for the estimated ethylene concentration, based on calculated solubilities in toluene (see Experimental Section).[26]

Only small differences between polymerization productivity were observed in the series **2a**−**e**. The chloro-substituted **2d** was significantly more productive at 60 °C than the other catalysts (Table 1, entry 19), while the polymerization rates at 80 °C were rather uniform across the series. At 115 °C, however, **2d** was again noticeably more active than the other catalysts. In general, no trend in polymerization rate with substituent can be discerned, aside from the higher productivity of catalyst **2d**.

Catalyst thermal stability was probed by running polymerizations for longer periods at 80 °C and comparing polymer yield to values predicted by simple extrapolation of the 10 min runs (Figure 1). The results do not illustrate a well-defined trend due to ligand substitution, as all catalysts afforded roughly equal productivities while still active. The most stable catalyst was CF_3-Cyc complex **2e**, which exhibited a 30 min productivity that was 25% less than the predicted value from 10 min extrapolation. Methyl-substituted **2c** was 40% deactivated after 30 min, and methoxy-substituted **2b** productivities appeared to level off entirely after 20 min, suggesting it underwent complete deactivation.

dx.doi.org/10.1021/om200193r |*Organometallics* 2011, 30, 2432–2452

Scheme 3. Synthesis of Cyclophane Ligands 1a−e

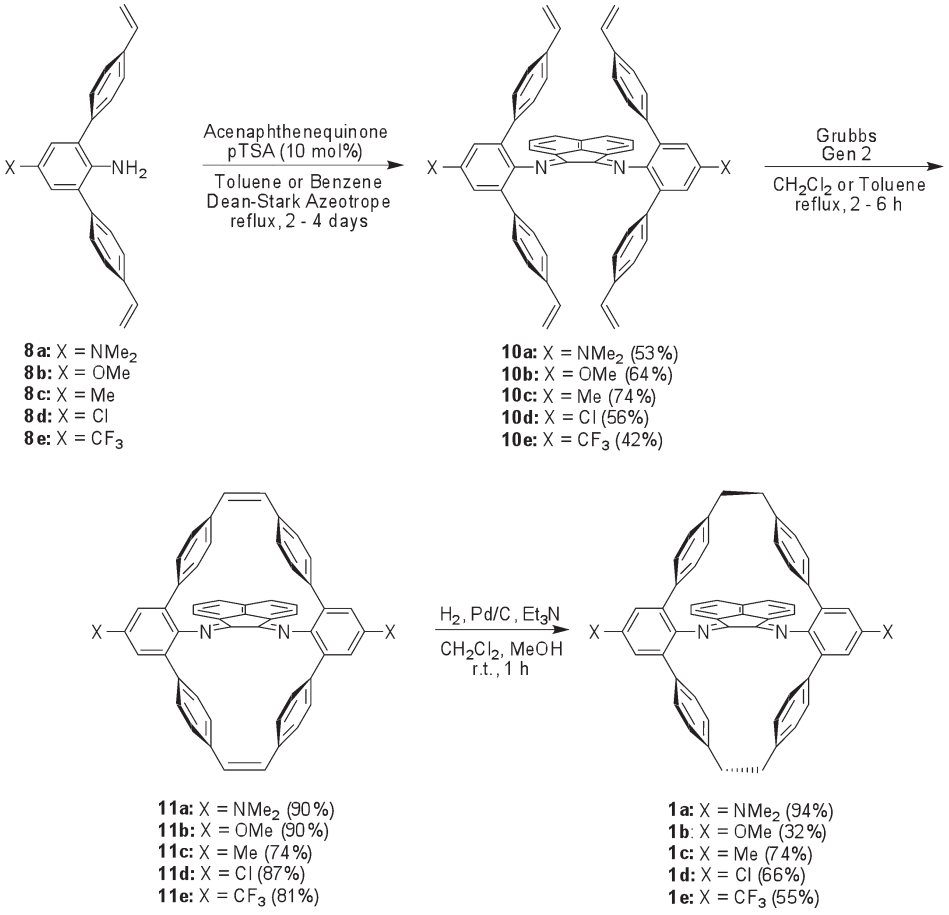

It is worth noting that the two most active catalysts, **2e** and chloro-substituted **2d**, were also the most thermally robust. Since there was no apparent polymerization rate acceleration after the first 10 min, one can assume that the catalysts were completely activated by then.

Although the reactivity of cyclophane-based Ni(II) catalysts **2a**−**e** showed no substantial differences, the polymers were produced with noticeable variations in molecular weight (Table 1). The polymers from the electron-rich catalysts **2a**−**c**, for example, generally exhibited lower molecular weights and higher polydispersities than the electron-poor catalysts **2d**,**e**. More importantly, molecular weights of polymers from the electron-poor catalysts, especially **2d**, grew larger as the polymerization duration increased from 10 to 30 min (entries 20−22). By comparison, only minor increases in molecular weight were noted at longer polymerization times with the electron-rich catalysts **2a**−**c**. These observations suggest that chain transfer may be more rapid for catalysts bearing more strongly electron-donating ligands, although catalyst stability is likely more influential. As discussed earlier, catalysts **2d**,**e**, for which an increase in number-average molecular weight (M_n) could be discerned over the course of a 30 min polymerization run, were also the most stable of the series. The microstructure of the polymers was deduced by differential scanning calorimetry (DSC) and ^{1}H NMR. In general, polymers prepared at 60 °C exhibited broad but pronounced melting peaks in DSC analysis. By 80 °C, the polymer melting temperature T_m was significantly reduced and the melting transitions were extremely broad and weak due to low polymer crystallinity. The catalysts seemed to afford polymer of similar properties with the exception of NMe_2-Cyc catalyst **2a**, which gave polymer of lowest branching density and high T_m. Polymers from **2a** were therefore more linear and crystalline than polymers from the other catalysts (Table 1, entry 3). This implied a reduced tendency for catalyst **2a** to undergo chain-walking isomerization compared to the other catalysts.

As an additional consideration, there exists the possibility that the NMe_2 and OMe groups on complexes **2a** and **2b** could be interacting with the aluminum activator, present as it is in such large excess. The formation of such a Lewis acid−base complex would be expected to reduce the electron-donating ability of these substituents and partially negate their affect. There is no conclusive evidence from the data that binding to the Al activator was observed, however.

Pd(II)-Substituted Cyclophane-Based Catalysts for Olefin Polymerization. Cyclophane-based Pd(diimine)MeCl complexes **3a**−**e** were prepared by displacement of benzonitrile from *in situ*-generated $Pd(PhCN)_2MeCl$ by variations of published procedures (Scheme 5).[20,27] Complexation of the unhydrogenated diimines **11b**−**e** to Pd(II) was carried out to prepare the complexes **14b**−**e**, which were then hydrogenated to the desired complexes **3b**−**e**. Unlike the free ligands, hydrogenation of the complexes required no added base to prevent over-reduction, presumably because of stabilization of the diimine by metal chelation. Attempted hydrogenation of the amino-substituted

dx.doi.org/10.1021/om200193r |*Organometallics* 2011, 30, 2432–2452

Scheme 4. Synthesis of [Ni(diimine)acac]$B(C_6F_5)_4$ Complexes 2a−e and Other Ni(II) Complexes Used in the Polymerization Study

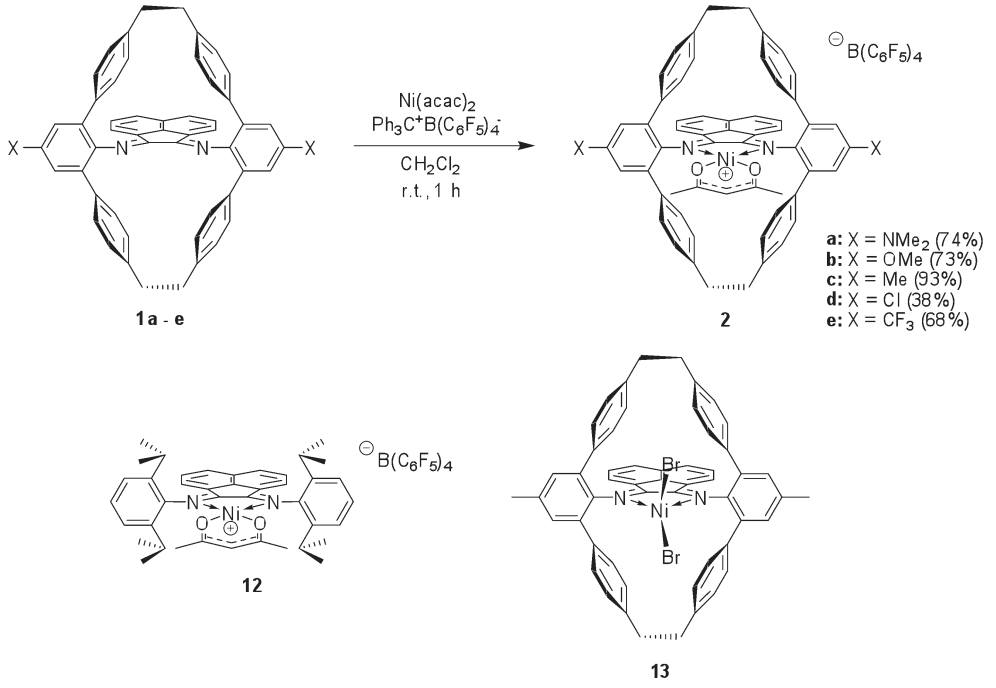

unsaturated Pd(II) complex **14a**, however, led to extensive decomposition that the presence of base could not prevent. In this case, the corresponding hydrogenated complex **3a** was prepared instead by complexation of prehydrogenated NMe_2-Cyc ligand **1a**.

As in our previous studies of substituted acyclic Pd(II) α-diimine complexes,[20,21] the nature of substituent influence on the electronics of Pd(II) cyclophane-based complexes was explored by NMR and infrared spectroscopy. The ^{1}H NMR chemical shifts of the Pd-bound methyl resonances for **3a**−**e** are plotted as a function of Hammett substituent constant σ_p[28] in Figure S2 in the Supporting Information. A trend of downfield shift for complexes bearing increasingly electron-donating groups was observed and attributed to deshielding by ring current of the phenyl rings. Similar but less pronounced magnetic anisotropy effects were also observed in the most electron-rich members of the acyclic series of complexes.[20]

Substituted cyclophane carbonyl complexes of Pd(II) **15a**−**e** were prepared by treatment of the methyl chlorides **3a**−**e** with sodium tetrakis(3,5-bis(trifluoromethyl)phenyl)borate (NaBAF) and CO (Scheme 6) in the manner previously described,[20] and the CO stretching frequency was measured by infrared spectrometry. The magnitude of perturbation of the CO bonding by the substituents is similar to that of the acyclic catalysts (Figure 2). Therefore, significant differences in catalyst activity and polymer properties should exist within this series of substituted cyclophane catalysts as well. Overall, the stretching frequencies of the cyclophane complexes are shifted at least 10 cm^{-1} to lower frequency compared to the acyclic complexes, indicating that metal back-bonding to CO is significantly increased. This observation also suggests that electron density on the metal is higher in the cyclophane complexes.

To probe the catalyst activity and thermal stability, experiments similar to those performed for the acyclic catalyst series[21] were conducted at 22 and 60 °C at ambient ethylene pressure, in which known volumes of the polymerization mixture were removed at 3, 6, and 20 h and dried, and the yield of polymer was measured. The complexes **3a**−**e** were all shown to polymerize ethylene upon activation with 1.5 equiv of NaBAF. For comparison, polymerization data for the unsubstituted acyclic complex **16** (Figure 3) are also given as a control. Plots of catalyst productivity versus time for these polymerizations are shown in Figure 4. Productivity in this case is not related to ethylene concentration since it is known that the polymerization rate of Pd(II) α-diimine catalysts is independent of olefin concentration.[5,7]

At 22 °C, nearly all of the catalysts were still partially active after 48 h. The only exception of stability was methoxy-substituted **3b**. Intrinsic activities could be gauged by measurement of polymer productivity after short polymerization times. While more active than the cyclophane-based catalysts, the acyclic catalyst **16** appeared to deactivate appreciably during the course of the polymerization run. Chloro-substituted **3d** was the most active cyclophane-based catalyst. At room temperature, the following activity trend was noted: acyclic > Cl > NMe_2 ∼ Me ∼ CF_3 > OMe.

At 60 °C, dimethylamino-substituted **3a** underwent rapid deactivation, as did its previously studied acyclic analogues.[20,21] Instability at high temperature appears to be a general phenomenon for the amino-substituted catalysts. The thermal sensitivity of the acyclic catalyst **16** was apparent compared to some of the cyclophane catalysts. Activities in general were dramatically higher than at room temperature, although stabilities were markedly decreased. The only catalyst that preserved the majority of its activity after 48 h was **3d**, which exhibited exceptional activity and stability. To the best of our knowledge, **3d** is the most active Pd(II) α-diimine catalyst to date at high temperatures. Polymerization at elevated temperature revealed the following trends in activity: Cl > CF_3 > OMe > Me ∼ acyclic > NMe_2, and thermal stability: Cl ≫ OMe ∼ Me ∼ CF_3 ∼ acyclic ≫ NMe_2.

dx.doi.org/10.1021/om200193r |*Organometallics* 2011, 30, 2432–2452

Table 1. Polymerization Results from Ni(II) α-Diimine Catalysts[a]

entry	complex	T (°C)	time (min)	yield (g)	productivity (kg mol^{-1} M^{-1})[b]	M_n (kg/mol)[c]	M_w/M_n[c]	B[d]	T_m (°C)[e]
1	**12**[f]	55	10	5.22	3600	214	1.5	56.9	
2	**12**[f]	70	10	1.22	1000	126	1.4	79.2	
3	**2a**	60	10	3.59	2600	325	2.2	79.6	114.5
4	**2a**	80	10	4.24	3600	246	1.7	94.2	93.2
5	**2a**	80	20	3.46[f]	5900	195	1.6		
6	**2a**	80	30	4.22[f]	7200	256	1.6		
7	**2a**	115	10	1.08	1200	118	1.5	103.0	
8	**2b**	60	10	5.28	3700	251	1.9	100.4	104.9
9	**2b**	80	10	4.26	3600	161	1.9	104.0	96.1
10	**2b**	80	20	4.06[f]	6900	178	1.7		
11	**2b**	80	30	4.10[f]	7000	189	1.7		
12	**2b**	115	10	0.84	2200	136	1.4	114.8	
13	**13**/MMAO	80	10	4.72	4100	235	1.7	112.2	
14	**2c**	60	10	4.30	3100	245	2.1	84.3	106.7
15	**2c**	80	10	4.52	3900	266	1.9	104.0	92.9
16	**2c**	80	20	2.96[f]	5100	276	1.8		
17	**2c**	80	30	3.84[f]	6600	266	1.9		
18	**2c**	115	10	0.92	1000	131	1.5	116.7	
19	**2d**	60	10	6.32	4600	310	2.2	101.9	114.9
20	**2d**	80	10	4.52	3900	229	1.7	118.1	85.2
21	**2d**	80	20	3.66[f]	6300	243	2.0		
22	**2d**	80	30	4.52[f]	7700	311	1.9		
23	**2d**	115	10	1.43	1600	143	1.5	122.4	
24	**2e**	60	10	5.20	3800	236	1.9	103.6	107.0
25	**2e**	80	10	4.26	3600	246	1.7	110.3	98.7
26	**2e**	80	20	3.98[f]	6800	250	1.6		
27	**2e**	80	30	4.74[f]	8100	278	1.6		
28	**2e**	115	10	1.04	1200	121	1.5	116.1	

[a] Polymerization conditions: 1.0 μmol of catalyst, 1500 equiv of TIBA (unless otherwise stated), 200 psi of ethylene. Solvent = 1,2-dichlorobenzene for runs > 80 °C, 4:1 toluene/1,2-dichlorobenzene for all other runs. [b] Productivity: kg of polymer per mole of catalyst per mol/L of ethylene. [c] Determined by GPC in 1,2,4-trichlorobenzene at 140 °C with polyethylene standards. [d] Branching density per 1000 carbons collected of polymers of 10 min runs at each temperature and determined by ^{1}H NMR. [e] Melting temperature of crystalline domains of polymers of 10 min runs, if detected by DSC analysis. [f] Catalyst load = 0.50 μmol.

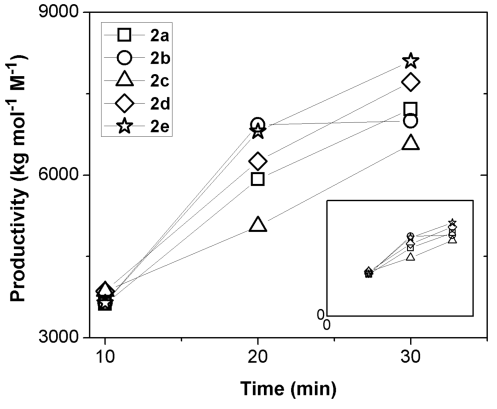

Figure 1. Plot of polymerization productivity versus time for catalysts **2a**−**e** activated with TIBA at 80 °C. The inset shows the full plot with the origin included.

The determination of M_n was carried out by size exclusion chromatography (SEC) using a multi-angle laser light scattering (MALLS) detector. Although the polymers produced by the cyclophane Pd(II) catalysts were all too small for accurate size (radius of gyration, R_g) measurement, MALLS provides accurate molecular weight regardless of the polymer branching topology.[29,30] Polymer molecular weight was found to increase with the use of more electron-withdrawing catalysts (Figure 5). Trifluoromethyl-substituted **3e** afforded polymer of up to 18 kg/mol, while the amino-substituted **3a** gave polymer of only one-third that mass at room temperature. This discrepancy increased to a 6-fold difference in molecular weight at 60 °C. This trend is opposite what was observed for the substituted acyclic Pd(II) catalysts,[21] where molecular weight was higher in polymers produced by electron-rich catalysts, and will be further elaborated in the Discussion section.

The physical properties of the polymers prepared by cyclophane catalysts **3a**−**e** and acyclic catalyst **16** were then examined (Table 2). The catalysts bearing electron-withdrawing groups exhibit polymer chain growth throughout the polymerization in addition to affording polymer of higher M_n. For example, catalyst **3a** showed only a moderate increase in M_n of 4.7 to 6.0 kg/mol from 3 to 48 h despite still remaining active during this time (Table 2, entry 2). In contrast, polymer prepared from catalyst **3e** exhibited a doubling of M_n from 9.2 to 17.9 kg/mol between 3

dx.doi.org/10.1021/om200193r |*Organometallics* 2011, 30, 2432–2452

Scheme 5. Synthesis of Pd(II) Cyclophane Methyl Chloride Complexes 3a−e

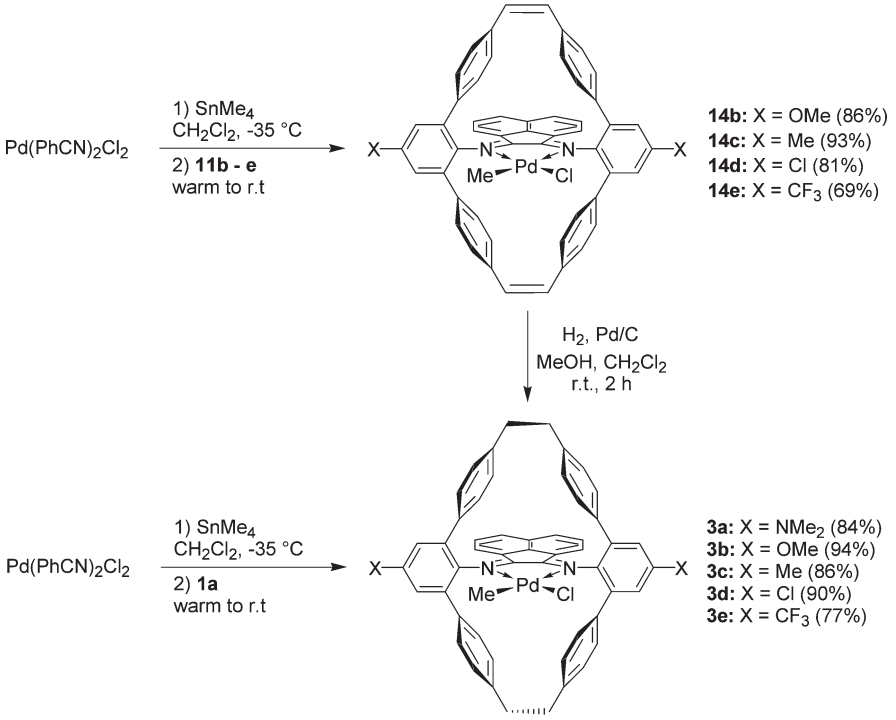

Scheme 6. Synthesis of Pd(II) Cyclophane Methyl Carbonyl Complexes 15a−e

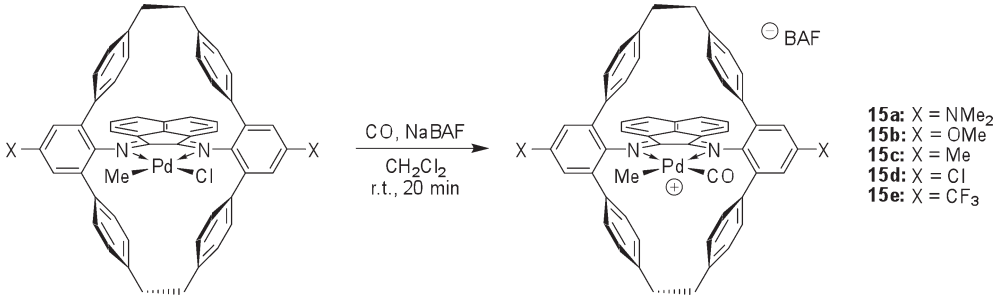

and 48 h (entry 6). Therefore, it can be concluded that chain transfer processes are significantly suppressed in catalysts bearing electron-withdrawing substituents.

To examine the effects of substitution on functional group tolerance and comonomer incorporation, copolymerizations were performed with the catalysts **3a**−**e** in the presence of 1.0 M methyl acrylate (MA) and 88 psi of ethylene (Table 3). A general trend of higher MA incorporation was measured by ^{1}H NMR in copolymer from increasingly electron-rich catalysts, which is consistent with the results from the acyclic series of catalysts.[20] The increased incorporation of MA corresponds precisely with a decrease in the stretching frequency of the corresponding carbonyl complex (see Figure 2). This observation supports the reasoning that MA incorporation levels are directly dependent on metal, and thus ligand, electronic properties. Incorporations of MA by the cyclophane catalysts were significantly higher than the analogous acyclic catalysts. It was mentioned above that carbonyl stretching frequencies in general were lower for the cyclophane complexes, implying an electron-rich metal center more accommodating to MA insertion. We have also previously identified another mechanistic origin of the elevated incorporation of acrylates by the Pd(II) cyclophane catalyst.[18,19] Higher levels of acrylate in copolymers with ethylene were shown to result from the ability of the cyclic ligand to restrict access of free olefin by blocking the axial coordination sites, thus interfering with monomer complexation equilibrium and reducing the usual preference for ethylene. The current observed behavior with MA incorporation is therefore consistent with the previously established trend in electronic effects and the behavior of the cyclophane ligand.

Polymer productivity is represented as molar turnover number in Table 3 to simplify comparison of the polymerization of the two different comonomers. In the acyclic series, the electron-rich catalysts, in addition to giving higher MA incorporation, also exhibited increased tolerance to acrylate incorporation in the form of higher activities and polymer molecular weight.[20] A similar trend was not observed for the cyclophane catalyst series. Instead, the higher MA incorportation with increasing electron-donating ability

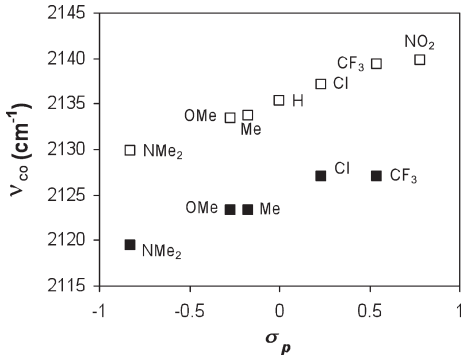

Figure 2. Plot of carbonyl IR stretching frequencies versus the *para*-Hammet substituent constant σ_p for cyclophane-based complexes **15a**−**e** (solid squares) and acyclic complexes (hollow squares, from ref 20).

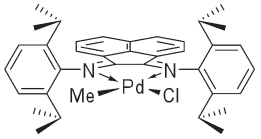

16

Figure 3. Unsubstituted acyclic Pd(II) α-diimine complex **16**.

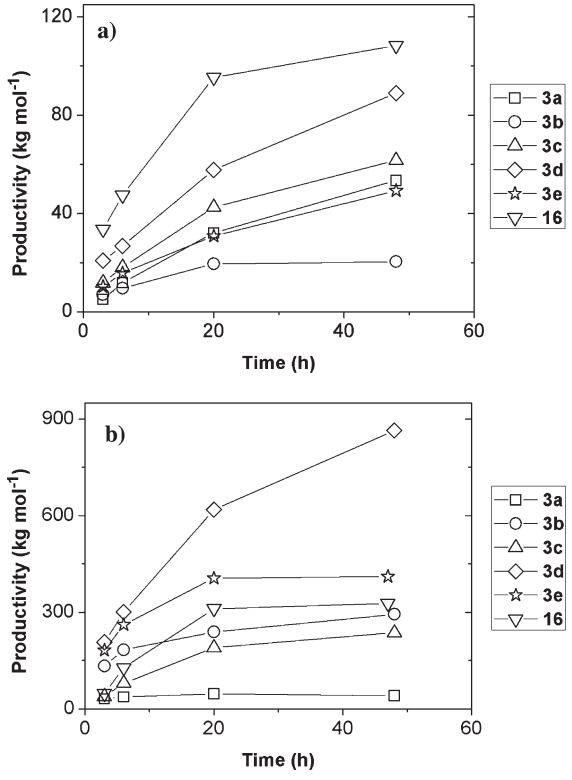

Figure 4. Plot of productivity versus time for complexes **3a**−**e** and **16** + NaBAF at (a) 22 °C and (b) 60 °C.

of the ligands was found to occur in conjunction with a reduction in polymer productivity. Catalyst **3a** was both the least active and afforded the lowest molecular weight polymer. On the other hand, chloro-substituted **3d** exhibited the highest activity and molecular

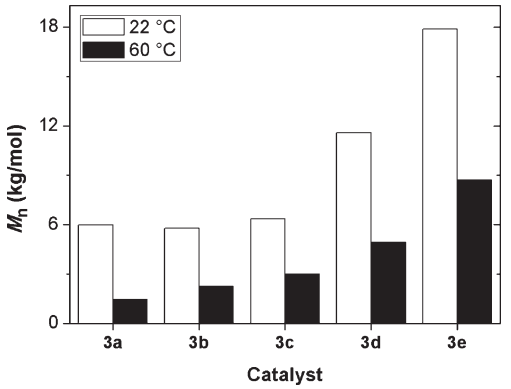

Figure 5. Number-average molecular weight (M_n) for polymers produced by catalysts **3a**−**e** + NaBAF after 48 h polymerizations at 22 and 60 °C.

weight. It was previously demonstrated that activity decrease occurs with increasing MA incorporation via the formation of stable chelate complexes after insertion of MA.[7] Although increased metal electron density favored the binding and incorporation of MA in the cyclophane system, it did not appear to help disrupt formation of this deactivating chelate intermediate.

DISCUSSION

Catalyst Productivity and Thermal Stability. Compared to the acyclic catalysts, the thermal stabilities of the cyclophane Ni(II) and Pd(II) systems were superior. This was especially evident in the Pd(II) series, where the rigidity of the cyclic structure was found to dramatically increase catalyst lifetime. Whereas the structurally similar but uncyclized terphenyl-based Pd(II) catalysts developed by Rieger and co-workers decomposed within minutes at room temperature,[31] Cl-Cyc catalyst **3d** was still active after two days at 60 °C (Figure 4). Interestingly, catalyst productivity and stability trends in the Pd(II) and Ni(II) cyclophane systems were opposite of what was seen for the acyclic catalyst series, in which the electron-rich catalysts were typically more robust.[21]

The dependence of productivity and thermal stability on substituent was complex, although electron-deficient catalysts generally outperformed the electron-rich analogues in the cyclophane system. In the Ni(II) cyclophane series, chloro-substituted catalyst **2d** was most productive, but CF_3-substituted **2e** was the most thermally stable. In the Pd(II) cyclophane series, although the CF_3-substituted Pd(II) complex **3e** appeared to have the highest intrinsic activity initially, chloro-substituted **3d** possessed greatly enhanced thermal stability. Even though the electron-deficient catalysts performed better overall than their electron-rich analogues, a metal center with excessively low electron density could be detrimental to reactivity. The superior performance of **3d** could result from a desirable balance in electronic properties.

Polymer Microstructure. Because the polymers produced by the Pd(II) cyclophane catalysts are of high branching density and low molecular weight, they are amorphous. The variation of branching density *B* does not appear to follow a noticeable trend. In fact, methyl-substituted **3c**, in the middle of the series, exhibits the lowest value of *B* at both ambient and high temperature (Table 2, entries 4 and 10). In the Ni(II) system, amino-substituted **2a** generally afforded polymer of lower branching density,

dx.doi.org/10.1021/om200193r |*Organometallics* 2011, 30, 2432–2452

Table 2. Properties of Polyethylene Prepared from Pd(II) Complexes 3a−e and 16[a]

				M_n (kg/mol)[c]				
entry	catalyst	T (°C)	3 h productivity (kg mol^{-1})[b]	3 h	48 h	M_w/M_n[d]	B[e]	catalyst lifetime (h)[f]
1	**16**	22	33.5	32.8	36.4	1.4	104.7	>48
2	**3a**	22	4.99	4.16	5.98	1.2	112.0	>48
3	**3b**	22	7.01	6.03	5.78	1.3	122.3	20
4	**3c**	22	11.8	6.30	6.37	1.4	108.9	>48
5	**3d**	22	20.7	7.69	11.6	1.4	120.4	>48
6	**3e**	22	10.2	9.20	17.9	1.4	117.0	>48
7	**16**	60	47.1	6.59	7.03	1.3	109.7	20
8	**3a**	60	30.5	1.46	1.46	1.5	127.6	6
9	**3b**	60	133	2.16	2.26	1.6	123.4	20
10	**3c**	60	38.7	2.92	3.00	1.6	116.0	20
11	**3d**	60	207	4.82	5.10	1.4	123.8	>48
12	**3e**	60	182	6.96	8.70	1.3	117.4	20

[a] Initial polymerization conditions: 20.0 μmol of catalyst and 1.5 equiv of NaBAF in 50 mL of toluene, 1 atm of ethylene pressure. Aliquots of 5 mL of the polymerization mixture were taken at 3, 6, and 20 h, and the remaining mixture was collected at 48 h. [b] Productivity: kg of polymer per mole of catalyst. [c] Number average molecular weight at 3 and 48 h polymerizations obtained from SEC-MALLS. [d] Polydispersity obtained from SEC-MALLS after 48 h. [e] Polymer branching density per 1000 carbons obtained from ^{1}H NMR at 48 h. [f] Catalyst lifetimes estimated from Figure 4.

Table 3. Copolymerizations of Ethylene and Methyl Acrylate (MA) from Pd(II) Acyclic Complex Cyclophane Complexes 3a−e and 16[a]

			turnover number[b]					
entry	catalyst	yield (mg)	C_2H_4	MA	mol % MA[c]	M_n (kg/mol)[d]	M_w/M_n[d]	B
1	**16**	340	1200	10	0.8	26.8	1.5	105
2	**3a**	39	101	12	10.9	4.16	1.3	126
3	**3b**	53	153	12	7.1	6.41	1.4	124
4	**3c**	49	141	11	7.1	5.80	1.5	120
5	**3d**	84	247	17	6.5	7.81	1.5	119
6	**3e**	73	214	15	6.5	5.04	1.3	129

[a] Polymerization conditions: 10.0 μmol of complex, 1.5 equiv of NaBAF, [MA] = 1.0 M, toluene solvent, 50 mL total reaction volume, 88 psi ethylene pressure, 25 °C, 18 h. [b] Turnover number: moles of monomer polymerized per mole of catalyst. [c] Determined by ^{1}H NMR. [d] Determined by MALLS.

higher polymer melting temperature, and higher crystallinity, all properties consistent with more linear polymer topology. The behavior for **2a** is expected since a less branched, more crystalline polymer implies less frequent chain walking, which is initiated by β-hydride elimination.[32] Hydride elminiation would be expected to occur with less facility due to stabilization of the electron-deficient reactive agostic intermediate. The effect is clearly, however, of minor importance.

As compared to the analogous acyclic catalysts, branching density is substantially higher in polymers produced by both the Ni(II) and Pd(II) cyclophane systems. Brookhart has observed a positive correlation between ligand steric bulk and branching density in polymers from Ni(II) α-diimine catalysts.[9] This trend was believed to result from reduced rates of trapping of the alkyl agostic intermediates because of increased ligand steric bulk preventing ethylene approach.[33] Because of the longer lifetime of the agostic intermediate, chain walking is more extensive in catalysts bearing bulker ligands. The same rationale would also explain higher branching degrees with the cyclophane Pd(II) catalyst as well, based on large amounts of evidence that suggests effective blocking of olefin monomer approach by the cyclophane ligand.[12,14,18,19] Previous studies by our laboratory on the polymerization of higher olefins by the cyclophane catalyst, notably the observation of a "chain-straightening" effect,[14] lend further support to accelerated chain walking in this system.

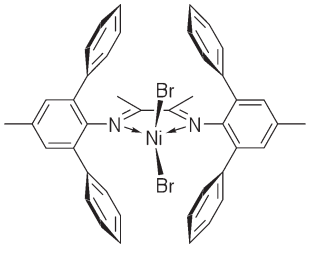

17

Figure 6. Nickel terphenyl-based complex **17**, from ref 25.

Comparison to the terphenyl-based Ni(II) catalysts developed by Rieger and co-workers, which lack the cyclic bridge but are otherwise analogous to the cyclophanes, further illustrate the sizable effect that ligand cyclization has on polymer microstructure.

Scheme 7. Preparation of Cyclophane-Based Pd(II) Acetonitrile and Dimethyl Sulfide Adducts 18 and 19

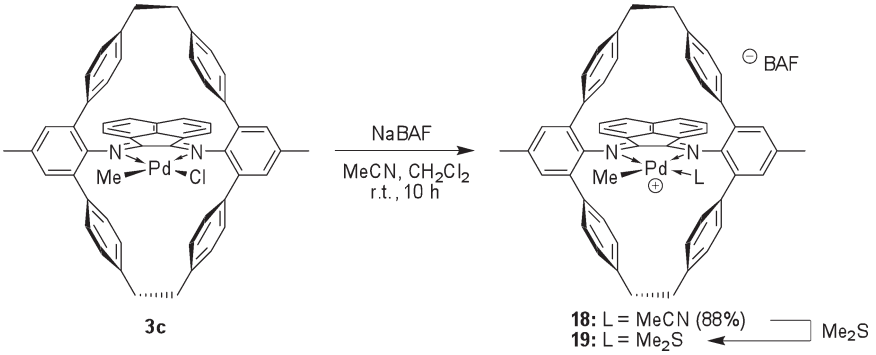

Scheme 8. Activation of 3c by NaBAF: Chloro-Bridged Dimer 20 and the Proposed Agostic Complex 21

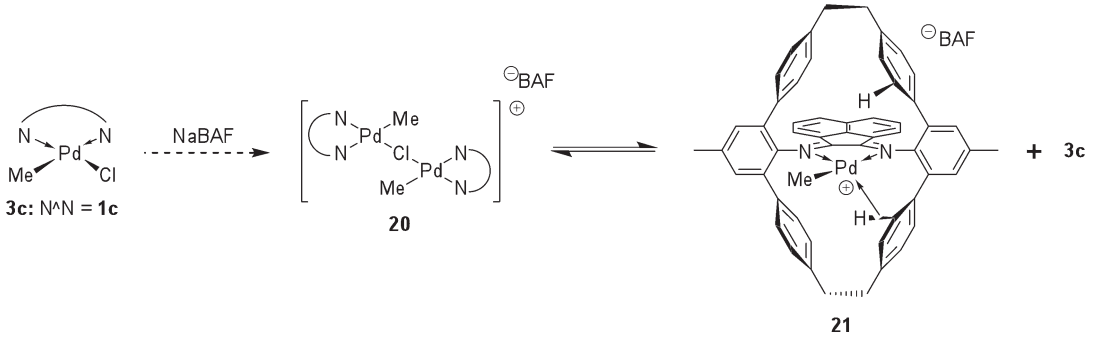

The Rieger system, of which complex **17** is typical (Figure 6), affords polymer of far higher linearity, attributable to the higher flexibility of that system that permits the complexation of ethylene at the expense of the chain-walking process.[25] By corollary, the rigidity provided by cyclization in the cyclophane catalysts discussed herein prevents disruptive ligand motions, leading to an environment conducive toward chain walking. Interestingly, chain walking has been described as a sterically demanding process,[29] and yet the cyclophane ligand system is able to accommodate it. The prevalence of chain walking in the present system most likely results from the aforementioned inhibition of ethylene complexation.

Evidence and Role of a Ligand−Metal H-Agostic Interaction. The Pd(II) cationic complexes are C_s symmetric, possessing only a plane of symmetry passing through the coordination plane, and thus exhibit eight doublets in the ^{1}H NMR spectrum corresponding to the 16 protons on the four axially oriented phenyl rings located above and below the metal coordination plane. The cationic Pd(II) adducts of the general formula [Pd(diimine)Me(L)]$^+$, where L is a strongly binding neutral ligand, exhibit this geometry and are suitable complexes for further study because of their stability and ease of formation. Thus the acetonitrile adduct **18** was prepared by reaction of **3c** with NaBAF in the presence of acetonitrile (Scheme 7). In addition, dimethyl sulfide adduct **19** was prepared *in situ* by reaction of **18** with one equivalent of Me_2S. Both complexes were stable as solutions in CH_2Cl_2 for days, allowing for detailed characterization under ambient conditions.

It was observed that upon formation of cationic cyclophane-based Pd(II) complexes such as **18** and **19**, one particular axial phenyl resonance in the ^{1}H NMR spectra underwent a significant upfield chemical shift by more than 1 ppm. This large upfield shift was first observed in the reaction of **3c** with NaBAF in the absence of a strongly binding neutral ligand, which is expected to produce the chloro-bridged dinuclear species [(Pd[Me-Cyc]-Me)$_2$(μ-Cl)]BAF **20** (Scheme 8), the acyclic analogue of which has been identified by Brookhart and co-workers.[10] Whereas this large chemical shift difference between neutral and cationic complexes could be due to an electrostatic effect from the buildup of positive charge at the metal, we propose here based on the evidence of upfield chemical shift an agostic-type ligand−metal interaction, represented in Scheme 8 by complex **21**, as a possible explanation. From the X-ray crystallographically derived structure of complex **3c**,[12] the axial phenyl rings are shown to be tipped toward the metal on the side of the chloro ligand, bringing the suspect hydrogen atoms close to the metal. The relatively close distance of 2.7 Å, measured between these hydrogen atoms and palladium in this neutral complex, suggests that an even closer approach to the metal is likely in cationic complexes, once loss of the chloro ligand occurs. Since these coordinatively unsaturated cationic complexes are important intermediates in the polymerization process, the potential of formation of a ligand−metal H-agostic interaction would have significant effects on the polymerization process. The rigid ligand geometry should prohibit the C−H bond from approaching the metal coordination plane in an equatorial interaction. Instead, a roughly axial H-agostic interaction is proposed, most likely involving the two front-side hydrogen atoms closest to the metal on the side of the neutral ligand or empty coordination site. Both of these hydrogen atoms are depicted in Scheme 8 as interacting

dx.doi.org/10.1021/om200193r |*Organometallics* 2011, 30, 2432–2452

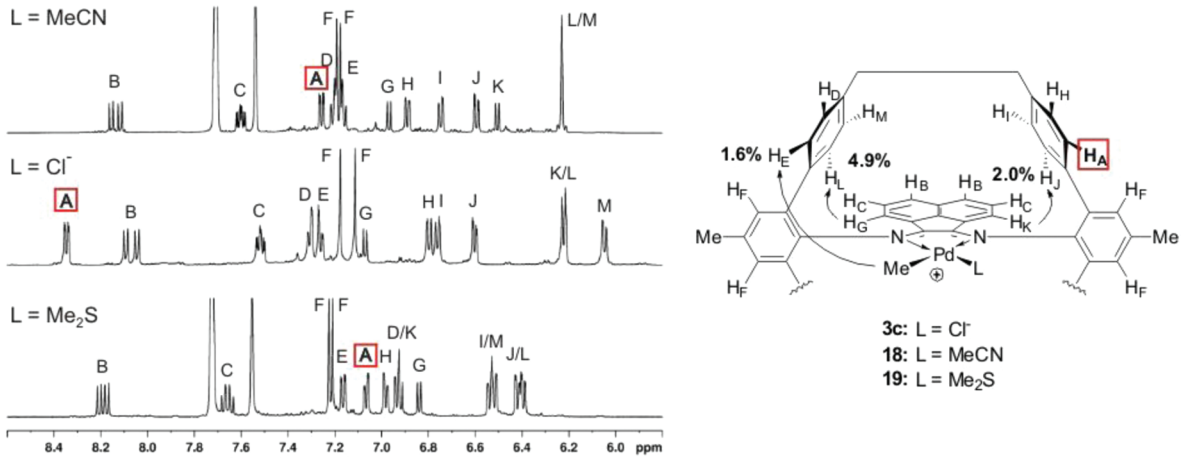

Figure 7. Aromatic proton assignments for complexes **3c**, **18**, and **19** corroborated by NOE and 2D NMR. NOE interactions are shown by the arrows, and percent enhancements are given for **3c**. The front, proximal, L-side hydrogen and its resonance are outlined by the square.

with the metal, which is possible considering the symmetry of the complex.

To gather further evidence to support the existence of an agostic-type interaction, the positions of the protons corresponding to the large upfield shifting resonance were identified by detailed NMR studies. Complexes **3c**, **18**, and **19** were fully assigned by 1D and 2D NMR methods (Figure 7). By irradiation of the Pd-Me group and acenaphthyl resonances, the unambiguous positions of the axial phenyl protons nearest to these groups were identified by NOE enhancement. Using COSY, HMBC, and HMQC methods, the remaining protons could be assigned on the basis of their positions relative to the NOE-enhanced protons. The close proximity of the methyl groups on the dimethyl sulfide ligand of **19** allowed for the direct determination of the nearest axial phenyl proton by NOE. The methyl group of acetonitrile in **18**, however, was too distant to lead to any NOE enhancements when irradiated. From the assignment, it was determined that the resonance undergoing the large upfield shift was indeed that of the protons nearest to the metal on the side of the neutral ligand. The shift of these two protons was far larger than that of any other aromatic resonance, as can be clearly seen in Figure 7.

Other metal−ligand interactions have importance in Pd(II) α-diimine polymerization catalysts. Products of C−H activation with *ortho*-isopropyl groups on the acyclic diimine ligands have been identified by Brookhart and are believed to be intermediates in catalyst decomposition.[10] The relative inaccessibility of ligand C−H bonds to the metal, such as in the *ortho*-dimethyl analogues or in ligands bearing less flexibility, likely imparts greater stability. The aforementioned family of terphenyl-based ligands developed by Rieger and co-workers form highly active Ni(II) catalysts such as complex **17** (Figure 6),[25] while the analogous Pd(II) catalyst **22** was much less stable than even the acyclic isopropyl-substituted catalyst **23** (Figure 8).[31] Since complex **23** differs from **22** only in the *ortho*-aryl functionality (phenyl versus isopropyl), the low stability of the terphenyl Pd(II) system likely stems from the *ortho*-phenyl groups. While activation of an alkyl C−H bond is involved in the case of the Brookhart-type acyclic catalyst, it is generally accepted that aryl C−H activation is more facile,[34−36] which presumably makes the terphenyl ligand system prone to accelerated decomposition. The rigidity of the cyclic cyclophane ligand, however, should hinder access of aryl C−H

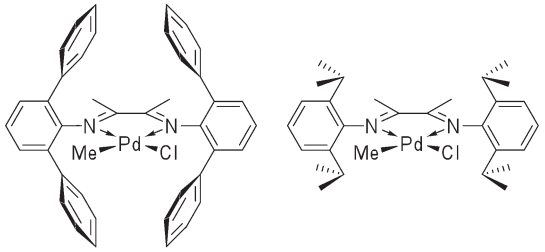

Figure 8. Terphenyl-based Pd(II) complex **22** (ref 31) and acyclic catalyst **23** (ref 3).

bonds to the metal center so that an agostic interaction is possible, but full bond cleavage is not favorable. This "hemilabile" agostic interaction would stabilize the reactive coordinatively unsaturated intermediate during polymerization. We have recently studied analogous Ni(II) and Pd(II) cyclophane-based catalysts with fluorine atoms in this position.[26] Significantly enhanced thermal stability was observed in the case of Ni(II), while the Pd(II) analogue exhibited a handful of properties suggestive of a related hemilabile interaction in this system. The proposed H-agostic interaction of the 14-electron intermediate **21** can explain some of the properties of the cyclophane catalyst system, such as the chain transfer process as discussed in the subsequent section.

Chain Transfer and Polymer Molecular Weight. With sufficient evidence supporting the role of the cyclophane ligand in suppressing the normal mode of chain transfer attributable to the bulkiness of the cyclophane ligand,[12,14,18,19] it comes as a surprise that molecular weights of polymers prepared by the Pd(II) catalyst are significantly lower than for the acyclic analogue. Although chain transfer must clearly be occurring to account for low polymer molecular weight, the processes involved must be different. The increased degree of chain walking discussed in the previous section may partly account for elevated chain transfer rates, as it implies that higher concentrations of the necessary olefin hydride intermediate exist. However, the bulky cyclophane ligand framework should significantly hinder the access of ethylene from axial sites and prevent normal modes of chain transfer via associative olefin substitution.

Scheme 9. Chain Transfer by Dissociation of the Olefin-Terminated Polymer from Complex 24 to Give Intermediate 25, the Ligand H-Agostic Form of Which Is Shown

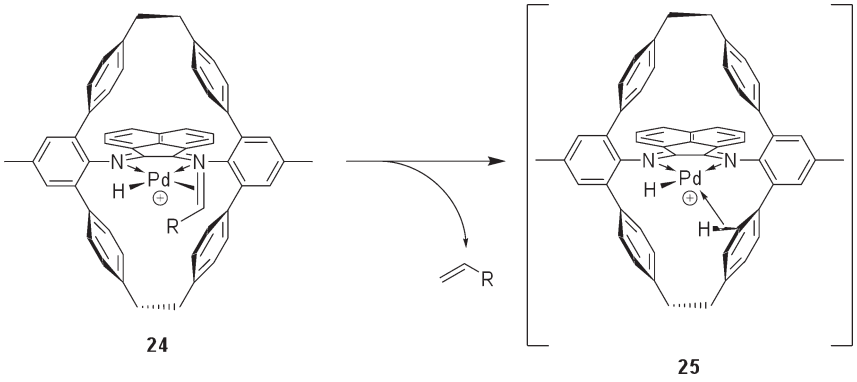

24 25

The generally accepted mechanism for chain transfer in square-planar d^8 complexes is through associative olefin substitution, in which a free olefin monomer has to first coordinate to the olefin hydride intermediate and then displace the polymeric olefin bound to the metal center. In a previous mechanistic investigation, we have elucidated that the energy barrier for ethylene exchange on the $[Pd(Me\text{-}Cyc)Me]^+$ complex is rather high: $\Delta G^{\ddagger} \approx 15.5$ kcal/mol under polymerization conditions.[19] This unusually high barrier is attributed to the difficulty of formation of the pentacoordinate transition state for associative substitution in the bulky cyclophane ligand environment. Since normal associative chain transfer processes involve a similar transition state, we had expected this process to be similarly retarded, which stands in contradiction to the relatively low molecular weight polymers obtained for the Pd(II) complexes.

A key finding of this study was the observation that polymer molecular weights increased with further ligand electron-withdrawing ability for the Pd(II) cyclophane-based system (Figure 5 and corresponding discussion). This trend was opposite of the previously studied acyclic system.[21] Thus a mechanistically different mode of ligand substitution that instead operates by a dissociative process was considered. Dissociative ligand substitution is generally unfavorable in square-planar d^8 complexes, such as those of Ni(II) and Pd(II). Rates of dissociative loss of bound ethylene in Pd(II) alkyl ethylene polymerization intermediates, for example, have been estimated to occur about 10^{10} times more slowly than associative exchange at −85 °C (at 1.0 M ethylene concentration this corresponds to a difference in $\Delta G^{\ddagger}$ of about 8.6 kcal/mol).[37] However, the entropy of activation of an associative process is large and negative; we determined an entropy of activation of −30 cal/mol·K for ethylene exchange in the cyclophane Pd(II) complex.[19] For a dissociative process, however, the entropy of activation is positive (+15 cal/mol·K is a typical value).[34] When adjusted to a polymerization temperature of 35 °C, the difference in $\Delta G^{\ddagger}$ between both processes (as determined from the relation $\Delta\Delta G^{\ddagger} = -\Delta T\Delta S^{\ddagger}$, dependence of $\Delta G^{\ddagger}$ on temperature for a particular process) is reduced by 5.4 kcal/mol to about 3.2 kcal/mol, corresponding to an associative to dissociative substitution rate ratio of only about 200. From studies of ethylene exchange rates with the Pd(II) cyclophane catalyst, it was concluded that associative exchange of ethylene was over 100 times slower for the cyclophane Pd(II) catalyst than the acyclic catalyst.[19] Taking all of these factors into consideration, the rates of associative and dissociative chain transfer could be quite comparable for the cyclophane Pd(II) complex.

In addition to the aforementioned considerations, a few other factors could further favor a dissociative chain transfer process. As illustrated in Scheme 9, dissociative chain transfer would proceed by dissociation of olefin-terminated polymer from olefin hydride intermediate **24**, an intermediate in the chain-walking process formed by β-hydride elimination from the 14 e^- polymerization intermediate. Previous studies have shown that dissociative exchange on group 10 metal complexes is usually promoted by electron-donating groups to better stabilize the highly electron-deficient 14 e^- intermediates.[38,39] Since we have established from characterization of the carbonyl complexes that the metal center is more electron rich in the cyclophane complexes than their acyclic analogues (Figure 2 and accompanying discussion), the rate of olefin dissociation could be increased by electronic stabilization of the coordinatively unsaturated intermediate hydride **25**. Compared to acyclic catalysts, previous experiments have shown that the complexation strength of ethylene is significantly reduced in cyclophane complexes,[19] presumably due to the more electron-rich metal center and larger steric hindrance. This effect would be further exacerbated by the larger size of the olefin-terminated polymer. In addition to the above arguments, the proposed ligand H-agostic interactions would further stabilize intermediate **25**, thus further facilitating olefin dissociation. For these reasons, dissociation of olefin-terminated polymer could be favorable enough to become the dominant chain transfer process and lead to a significant reduction of polymer molecular weight. Polymerization of a new chain can then resume upon complexation of ethylene to **25**, leading to hydride insertion and an intermediate analogous to **21**.

In the case of the Ni(II) catalysts, olefin dissociation has already been considered an important chain transfer mechanism from computational calculations.[40] Therefore, the less pronounced but otherwise analogous ligand electronic effect trends in polymer molecular weight in the Ni(II) cyclophane catalyst series can be explained by the same phenomenon.

CONCLUSION

A systematic investigation of ligand substitution effects on a family of cyclophane-based Ni(II) and Pd(II) catalysts was performed. The ligands were synthesized by a simplified route involving a one-step preparation of the *meta*-terphenyl ani-

lines by Suzuki coupling of a substituted dibromoaniline with 4-vinylphenylboronic acid. Ligand synthesis following this step was analogous to the standard procedure, aside from slight modification. The complexation to Ni(II) was efficiently carried out by reaction of the diimines to $Ni(acac)_2$ in the presence of trityl cation. Polymerizations could be initiated by activation of the resulting cationic Ni(diimine)acac complexes with MMAO, trimethylaluminum, and triisobutylaluminum. The Pd(II) complexes were all prepared by substitution onto *in situ*-generated $Pd(PhCN)_2MeCl$. Polymerizations with these complexes were activated by the addition of NaBAF. Key findings from this study were as follows:

(1) From measurement of the CO ligand stretching frequencies of the Pd(II) methyl carbonyl complexes of the cyclophane ligands, the introduction of substituents was found to affect the electron density of the metal. The magnitude of the perturbation is similar to that in the acyclic complexes studied previously.[20,21] The cyclophane complexes exhibited a CO stretching frequency at least 10 cm^{-1} lower than the analogous acyclic complexes. This observation suggested that the metal center of a cyclophane complex is comparatively electron rich.

(2) The Ni(II) polymerizations of ethylene at high temperature were relatively insensitive to electronic perturbation, affording polyethylene in slightly increasing activity and thermal stability in the presence of ligand electron-withdrawing groups. At the same time, molecular weights increased as metal electron density decreased. The polymers were heavily branched and of low crystallinity.

(3) Electronic effects in the Pd(II) series of cyclophane catalysts were significant, but no discernible trend in activity or thermal stability was observed. The chloro-substituted cyclophane catalyst alone exhibited exceptionally high activity and stability at temperatures as high as 60 °C. In contrast, the polymer molecular weight dependence on substituent was pronounced and easily related to the electronic properties of the substituent. More electron-deficient catalysts afforded polymer with significantly higher molecular weight, which is the opposite trend of that noted for the acyclic catalysts.

(4) From detailed spectroscopic studies of the Pd(II) cyclophane complexes, evidence for an additional interaction between the cyclophane ligand and the metal was gathered. One particular aromatic resonance, corresponding to hydrogen located on the aryl rings near possible metal axial coordination sites, underwent a dramatic chemical shift upon transformation of a neural Pd(II) complex into a cationic one. An H-agostic interaction is proposed to account for this observation, which would act to stabilize coordinatively unsaturated intermediates and increase the thermal stability of the catalysts.

(5) To account for a number of unexpected observations in molecular weight trends, including the surprisingly low molecular weight for the bulky cyclophane-Pd(II) catalysts and the unexpected trend that higher molecular weight polymers were prepared by more electron-deficient catalysts, a new dissociative chain transfer mechanism was proposed. On the basis of reasonable estimates of dissociative ligand exchange rates, and in light of the observation that associative exchange processes are greatly retarded, the dissociative chain transfer mechanism may become the dominant mode of chain transfer. The stronger electron-donating ability of the cyclophane ligand, larger steric repulsion, and the contribution from the ligand H-agostic interaction all facilitate the dissociation of the complexed olefin-terminated polymer, thus promoting dissociative chain transfer.

EXPERIMENTAL SECTION

General Considerations. All catalyst handling was carried out in a Vacuum Atmospheres glovebox filled with nitrogen. All moisture- and air-sensitive reactions were carried out in flame-dried glassware using magnetic stirring under a positive pressure of nitrogen. Removal of organic solvents was accomplished by rotary evaporation and is referred to as concentrated *in vacuo*. Flash column chromatography was performed using forced flow on 230−400 mesh silica gel purchased from Dynamic Adsorbents, Inc. NMR spectra were recorded on Bruker DRX400, DRX500, and AVANCE600 FT-NMR instruments. Proton and carbon NMR spectra were recorded in ppm and were referenced to the indicated solvents. Boron-11 and fluorine-19 NMR spectra were recorded in ppm and were referenced to BF_3-diethyl etherate and $CFCl_3$, respectively. Data was reported as follows: chemical shift, multiplicity (s = singlet, d = doublet, t = triplet, q = quartet), integration, and coupling constant(s) in hertz (Hz). Multiplets (m) were reported over the range (ppm) at which they appear at the indicated field strength. Elemental analysis was performed by Atlantic Microlab, Norcross, GA. High-resolution mass spectrometry (HR-MS) was recorded on a Micromass LCT or Micromass Autospec. Infrared spectrometry was performed by the thin film method with a Prospect PRS-102 spectrometer from Midac Corp. High-pressure polymerizations were conducted in a mechanically stirred, water-cooled, 600 mL Parr autoclave. Polymer melting transitions were measured by a TA Instruments Q100 differential scanning calorimeter at UCI's California Institute of Telecomunications and Information Technology (CalIT2) materials characterization facility. Ethylene solubilities at desired pressures and temperatures were calculated by fitting techniques[26] based on experimental values reported by Lee et al. in toluene.[41]

Materials. Toluene, tetrahydrofuran (THF), diethyl ether, and dichloromethane were purified by passing through solvent purification columns[42] and are referred to herein as dry. Pentane was dried by distillation from the solution with sodium and benzophenone. 1,2-Dichlorobenzene was purified by passage through basic alumina under a nitrogen atmosphere. Unless otherwise stated, all other solvents and reagents were purchased from commercial suppliers and used as received. All catalysts were stored in a glovebox under a nitrogen atmosphere. The syntheses and characterization of all methyl-substituted cyclophane ligands and derivatives (except Ni(II) complex **2c** and Pd(II) complexes **18** and **19**),[12,13] aniline **4b**,[22] 2-dicyclohexylphosphino-2′,6′-dimethoxybiphenyl (S-Phos),[23] and sodium tetrakis(3,5-bis(trifluoromethyl)-phenyl)borate (NaBAF)[43] were prepared by known literature procedures. Spectral data for the BAF counterion can be found elsewhere and will not be repeated in the spectroscopic data below.[7] Methyl acrylate (Aldrich, 99%) was used as received.

1,3-Dibromo-5-fluoro-2-nitrobenzene (6). To a solution of 9.55 g of 2,6-dibromo-4-fluoroaniline **5** (35.5 mmol) in 200 mL of CH_2Cl_2 was added 35.02 g of 3-chloroperoxybenzoic acid (142 mmol, 70% by weight). The mixture was heated to reflux and stirred for 5 h. The reaction mixture was cooled to 0 °C in an ice bath, then filtered. The filtrate was then washed with 1.0 N KOH (3 × 150 mL), and the organic layer was concentrated *in vacuo* to afford a brown solid. The residue was dissolved in 100 mL of glacial acetic acid. To this solution was added 50 mL of a 30% H_2O_2 solution and 8 mL of concentrated nitric acid. The mixture was heated to reflux and stirred for 3 h, then poured into 500 mL of ice water and left to stand overnight at 4 °C. The suspension was filtered and the solid washed with water, then dried on the filter under air

suction for 2 h. The solid was recrystallized in hexanes to afford **6** as tan crystals (7.76 g, 73%): ^{1}H NMR (600 MHz, $CDCl_3$) δ 7.41 (d, 2H, J_{HF} = 7.4 Hz); ^{13}C NMR (125 MHz, $CDCl_3$) δ 114.9 (d, $^3J_{CF}$ = 11.3 Hz), 120.4 (d, $^2J_{CF}$ = 26.4 Hz), 148.8, 161.5 (d, $^1J_{CF}$ = 260.4 Hz). Anal. Calcd for $C_6H_2NO_2FBr_2$: C, 24.11; H, 0.67; N, 4.69. Found: C, 24.38; H, 0.67; N, 4.54.

3,5-Dibromo-*N*,*N*-dimethyl-4-nitroaniline (7). To a solution of 7.70 g of **6** (25.8 mmol) and 7.12 g of K_2CO_3 (51.5 mmol) in 30 mL of DMSO was added 15.5 mL of dimethylamine solution in methanol (2.0 M, 30.9 mmol). The mixture was stirred at room temperature for 3.5 h, then poured into 400 mL of 0.25 N NaOH solution. The resulting mixture was left to stand for 4 h at 4 °C and filtered, and the solid rinsed with water. Recrystallization in ethanol afforded **7** as rust-colored crystals (7.28 g, 87%): ^{1}H NMR (500 MHz, $CDCl_3$) δ 6.74 (s, 2H), 3.02 (s, 6H); ^{13}C NMR (125 MHz, $CDCl_3$) δ 40.2, 114.1, 115.0, 140.7, 151.2. Anal. Calcd for $C_8H_8N_2O_2Br_2$: C, 29.66; H, 2.49; N, 8.65. Found: C, 29.69; H, 2.46; N, 8.54.

2,6-Dibromo-4-(*N*,*N*-dimethylamino)aniline (4a). To a suspension of 5.113 g of **7** (15.78 mmol) and tin(II) chloride dihydrate (16.02 g, 71.02 mmol) in 120 mL of 2-propanol and 30 mL of $CHCl_3$ was added 20 mL of concentrated HCl. The mixture was heated to reflux with stirring for 5 h and cooled, the organic solvent was removed *in vacuo*, and water (200 mL) was added to the residue. Solid KOH was added until the mixture was strongly basic. The mixture was extracted with CH_2Cl_2, and the organic layers were concentrated *in vacuo*. The residue was dissolved in 50 mL of ethanol and 25 mL of water, heated until homogeneous, then concentrated *in vacuo* until needle-like crystals appeared. The mixture was then left to stand at 4 °C overnight, filtered, then dried to afford **4a** as pale yellow needles (4.20 g, 91%): ^{1}H NMR (500 MHz, $CDCl_3$) δ 6.87 (s, 2H), 4.06 (br s, 2H), 2.81 (s, 6H); ^{13}C NMR (125 MHz, $CDCl_3$) δ 41.6, 110.5, 117.6, 133.5, 145.1; HR-MS calcd for $[C_8H_{10}N_2Br_2 + H]^+$ 292.9283, found 292.9285.

4-Vinylphenylboronic Acid (9). This compound was prepared in a similar manner to that reported by Dale and Rush.[44] To a solution of trimethyl borate (16.1 mL, 14.7 g, 142 mmol) in 120 mL of dry THF cooled to −45 °C was dropwise added a solution of 4-vinylphenylmagnesium chloride (prepared from 2.026 g of magnesium powder and 10.0 mL (11.6 g, 83.3 mmol) of 4-chlorostyrene) in 40 mL of dry THF. After addition was complete, the mixture was slowly warmed to room temperature over 3 h and then quenched with 320 mL of 3.0 N HCl. The organic layer was set aside, and the aqueous layer was extracted with diethyl ether (2 × 100 mL). The organic phases were combined and concentrated *in vacuo*, 200 mL of water added, and the mixture was heated to boiling. The mixture was decanted, and the residual solid treated with an additional 100 mL of water, heated to boiling, and again decanted. The supernatants were combined and allowed to cool to room temperature, then stored at 4 °C for 4 h. The mixture was filtered, and the solid washed with water, then dried under soft vacuum overnight at room temperature to afford **9** as white crystals (11.90 g, 97%): ^{1}H NMR (500 MHz, $CDCl_3$) δ 5.28 (d, 1H, J = 10.9 Hz), 5.87 (d, 1H, J = 17.6 Hz), 6.73 (dd, 1H, J = 17.6, 10.9 Hz), 7.42 (d, 2H, J = 7.9 Hz), 7.77 (d, 2H, J = 8.0 Hz), 8.01 (br s, 2H); ^{11}B NMR (160 MHz, $CDCl_3$) δ 29.19 (br).

2,6-(4′-Vinylphenyl)-4-(*N*,*N*-dimethylamino)aniline (8a). A mixture of **9** (2.02 g, 13.7 mmol), 1.96 g of **4a** (6.14 mmol), and 6.28 g of finely ground $K_3PO_4 \cdot H_2O$ (27.3 mmol) in THF (150 mL) and water (3.0 mL) was degassed under a nitrogen stream for 20 min. To this were added 56 mg of S-Phos (0.14 mmol) and 31 mg of $Pd(OAc)_2$ (0.14 mmol), and the mixture was heated to reflux and stirred overnight. After filtration through Celite, 50 mL of saturated NH_4Cl solution and water (100 mL) were added, and the mixture was extracted with diethyl ether (2 × 150 mL). The organic layers were combined, washed with brine, and dried over $MgSO_4$. Purification by flash chromatography with 5% ethyl acetate in hexanes afforded **8a** as a bright yellow solid, identifiable by yellow fluorescence at 365 nm (1.561 g, 75%): ^{1}H NMR (500 MHz, $CDCl_3$) δ 2.91 (s, 6H), 3.72 (br s, 2H), 5.30 (d, 2H, J = 10.9 Hz), 5.81 (d, 2H, J = 17.6 Hz), 6.73−6.81 (m, 4H), 7.51 (pseudo s, 8H); ^{13}C NMR (125 MHz, $CDCl_3$) δ 42.6, 114.3, 116.8, 126.8, 129.0, 129.7, 136.62, 136.80, 139.8; HR-MS calcd for $[C_{24}H_{24}N_2 + H]^+$ 341.2018, found 341.2010.

2,6-(4′-Vinylphenyl)-4-methoxyaniline (8b). To a solution of 6.00 g of anhydrous $ZnCl_2$ (44.0 mmol) in dry THF (50 mL) at 0 °C was added 4-vinylphenylmagnesium chloride, prepared from 5.28 mL of 4-chlorostyrene (6.10 g, 44.0 mmol) and 1.070 g of magnesium powder (44.0 mmol). The suspension was warmed to room temperature, stirred for 2 h, then transferred via cannula to a solution of 2,6-dibromo-4-methoxyaniline (**4b**) (4.943 g, 17.59 mmol), 144 mg of S-Phos (0.352 mmol), and 161 mg of $Pd_2(dba)_3$ (0.176 mmol) in 50 mL of dry THF. The mixture was heated to reflux and stirred overnight, cooled, and then quenched with water (50 mL) and saturated NH_4Cl solution (50 mL). The organic phase was separated and set aside, and the aqueous phase was extracted with diethyl ether (2 × 50 mL). The organic phases were combined, washed with brine, and then dried over $MgSO_4$. Purification by flash chromatography in 2% ethyl acetate in hexanes, followed by further recrystallization in hexanes, afforded **8b** as a white solid, identifiable by pale blue fluorescence at 365 nm (2.700 g, 47%): ^{1}H NMR (500 MHz, $CDCl_3$) δ 3.57 (br s, 2H), 3.80 (s, 6H), 5.30 (d, 2H, J = 10.9 Hz), 5.81 (d, 2H, J = 17.6 Hz), 6.76 (s, 2H), 6.77 (dd, 2H, J = 17.6, 10.9 Hz), 7.51 (pseudo s, 8H); ^{13}C NMR (100 MHz, $CDCl_3$) δ 56.1, 114.4, 115.6, 122.7, 126.9, 129.05, 129.68, 136.61, 136.92, 139.4, 152.5.

2,6-(4′-Vinylphenyl)-4-chloroaniline (8d). A mixture of **9** (2.00 g, 13.5 mmol), 1.73 g of **4d** (6.06 mmol), and 6.24 g of finely ground $K_3PO_4 \cdot H_2O$ (27.1 mmol) in THF (130 mL) and water (3.0 mL) was degassed under a nitrogen stream for 20 min. To this was added 56 mg of S-Phos (0.14 mmol) and 30 mg of $Pd(OAc)_2$ (0.14 mmol), and the mixture was heated to reflux and stirred overnight. After filtration through Celite, 50 mL of saturated NH_4Cl solution and water (100 mL) were added, and the mixture was extracted with diethyl ether (2 × 150 mL). The organic layers were combined, washed once with water and twice with brine, and dried over $MgSO_4$. Purification by flash chromatography with 1% ethyl acetate in hexanes afforded **8d** as a white solid, identifiable by pale blue fluorescence at 365 nm (1.533 g, 76%): ^{1}H NMR (500 MHz, $CDCl_3$) δ 3.82 (br s, 2H), 5.30 (d, 2H, J = 10.9 Hz), 5.81 (d, 2H, J = 17.6 Hz), 6.75 (dd, 2H, J = 17.6, 10.9), 7.09 (s, 2H), 7.43 (d, 4H, J = 8.2 Hz), 7.50 (d, 2H, J = 8.1 Hz); ^{13}C NMR (100 MHz, $CDCl_3$) δ 114.7, 123.0, 127.0, 129.09, 129.29, 129.55, 136.5, 137.2, 138.2, 139.8; HR-MS calcd for $[C_{22}H_{18}NCl + H]^+$ 332.1206, found 332.1213.

2,6-(4′-Vinylphenyl)-4-(trifluoromethyl)aniline (8e). A mixture of **9** (3.00 g, 20.3 mmol), 1.94 g of **4e** (9.12 mmol), and 9.36 g of finely ground $K_3PO_4 \cdot H_2O$ (40.7 mmol) in THF (200 mL) and water (4.0 mL) was degassed under a nitrogen stream for 20 min. To this were added 83 mg of S-Phos (0.21 mmol) and 46 mg of $Pd(OAc)_2$ (0.21 mmol), and the mixture was heated to reflux and stirred overnight. After filtration through Celite, 50 mL of saturated NH_4Cl solution and water (100 mL) were added, and the mixture was extracted with diethyl ether (2 × 150 mL). The organic layers were combined, washed with brine, and dried over $MgSO_4$. Purification by flash chromatography with 5% ethyl acetate in hexanes afforded **8e** as a white solid, identifiable by pale blue fluorescence at 365 nm (2.958 g, 89%): ^{1}H NMR (500 MHz, $CDCl_3$) δ 4.15 (br s, 2H), 5.31 (d, 2H, J = 10.9 Hz), 5.82 (d, 2H, J = 17.6 Hz), 6.76 (dd, 2H, J = 17.6, 10.9 Hz), 7.35 (s, 2H), 7.44 (d, 4H, J = 8.2 Hz) 7.52 (d, 4H, J = 8.2 Hz); ^{13}C NMR (125 MHz, $CDCl_3$) δ 114.6, 119.8 (q, $^2J_{CF}$ = 32.7 Hz), 124.8 (q, $^1J_{CF}$ = 270.4 Hz), 126.5 (q, $^3J_{CF}$ = 3.8 Hz), 126.9, 127.1, 129.3, 136.2, 137.23, 137.79, 144.0; HR-MS calcd for $[C_{23}H_{18}NF_3 + H]^+$ 366.1470, found 366.1468.

General Procedure for Diimine Condensation (refs 29, 45). *para*-Toluenesulfonic acid monohydrate (pTSA, 10 mol % with respect

to aniline) was added to a suspension of aniline, acenaphthenequinone (0.45 equiv), and 1 mg of 4-methoxyphenol (to inhibit polymerization of the styryl group) in toluene or benzene. The flask was fitted with a 20 mL Dean−Stark trap filled with $MgSO_4$ and layered on top with 4 Å molecular sieves, a condenser. The mixture was heated to reflux for 2 to 4 days and then cooled, concentrated *in vacuo*, and purified accordingly.

Open NMe_2-Diimine (10a). Following the general procedure for diimine condensation, aniline **8a** (1.672 g, 4.91 mmol), acenaphthenequinone (403 mg, 1.96 mmol), and 100 mg of pTSA were reacted in 40 mL of toluene for 2 days, then purified by flash chromatography in 7:1 hexanes/ethyl acetate to afford **10a** as a burgundy solid (973 mg, 53%): ^{1}H NMR (400 MHz, $CDCl_3$) δ 3.07 (s, 12H), 5.16 (d, 4H, J = 10.9 Hz), 5.63 (d, 4H, J = 17.6 Hz), 6.60 (dd, 4H, J = 17.6, 10.9 Hz), 6.87 (s, 4H), 6.91 (d, 2H, J = 7.2 Hz), 7.07−7.13 (m, 10H), 7.38 (d, 2H, J = 8.2 Hz), 7.50 (d, 8H, J = 8.2 Hz); ^{13}C NMR (100 MHz, $CDCl_3$) δ 41.2, 113.5, 115.4, 122.2, 125.7, 127.24, 127.92, 129.81, 129.98, 130.3, 132.2, 135.7, 136.8, 138.0, 140.5, 148.2, 161.4; HR-MS calcd for $[C_{60}H_{50}N_4 + H]^+$ 827.4114, found 827.4110.

Open OMe-Diimine (10b). Following the general procedure for diimine condensation, aniline **8b** (2.681 g, 8.19 mmol), acenaphthenequinone (672 mg, 1.96 mmol), and 100 mg of pTSA were reacted in 40 mL of toluene for 2 days. The reaction was allowed to cool, upon which an orange solid precipitated. Diethyl ether (50 mL) was added, and the mixture cooled to −35 °C for 6 h and filtered through a plug composed of silica gel above Celite. The filtrate was set aside, and the solid was recovered in CH_2Cl_2 and concentrated to afford **10b** as an orange solid (1.409 g). The filtrate was concentrated *in vacuo*, then purified by flash chromatography in 6:1 hexanes/ethyl acetate. Additional product crystallized from the eluted fractions, which were concentrated and filtered to afford another 486 mg of **10b** of analytical purity (64% total): ^{1}H NMR (500 MHz, $CDCl_3$) δ 3.93 (s, 6H), 5.14 (d, 4H, J = 10.9 Hz), 5.59 (d, 4H, J = 17.7 Hz), 6.55 (dd, 4H, J = 17.6, 11.0 Hz), 6.80 (d, 2H, J = 7.2 Hz), 6.97 (s, 4H), 7.03 (d, 8H, J = 8.1 Hz), 7.18 (t, 2H, J = 8.1 Hz), 7.43 (d, 8H, J = 8.1), 7.54 (d, 2H, J = 8.3 Hz); ^{13}C NMR (100 MHz, $CDCl_3$) δ 55.9, 113.8, 115.9, 122.5, 125.9, 127.4, 128.3, 129.75, 129.80, 130.4, 132.5, 136.05, 136.73, 139.6, 140.30, 140.73, 156.9, 161.5; HR-MS calcd for $[C_{58}H_{44}N_2O_2 + H]^+$ 801.3481, found 801.3478.

Open Cl-Diimine (10d). Following the general procedure for diimine condensation, aniline **8d** (1.553 g, 4.62 mmol), acenaphthenequinone (379 mg, 2.08 mmol), and 80 mg of pTSA were reacted in 120 mL of toluene for 2 days, then purified by flash chromatography in 19:1 hexanes/ethyl acetate to afford **10d** as an orange solid (942 mg, 56%): ^{1}H NMR (500 MHz, $CDCl_3$) δ 5.12 (d, 4H, J = 11.0 Hz), 5.57 (d, 4H, J = 17.6 Hz), 6.51 (dd, 4H, J = 17.6, 11.0 Hz), 6.78 (d, 2H, J = 7.2 Hz), 7.02 (d, 8H, J = 8.2 Hz), 7.20 (t, 2H, J = 8.1 Hz), 7.37−7.40 (m, 12H), 7.55 (d, 2H, J = 8.3 Hz); ^{13}C NMR (100 MHz, $CDCl_3$) δ 114.0, 122.5, 125.9, 127.4, 128.29, 128.63, 129.10, 129.27, 129.47, 129.87, 130.10, 130.32, 132.7, 136.37, 136.42, 145.4, 160.6; HR-MS calcd for $[C_{56}H_{38}N_2Cl_2 + H]^+$ 809.2490, found 809.2487.

Open CF_3-Diimine (10e). Following the general procedure for diimine condensation, aniline **8e** (1.312 g, 3.59 mmol), acenaphthenequinone (294 mg, 1.61 mmol), and 70 mg of pTSA were reacted in 20 mL of benzene for 4 days, then purified by flash chromatography in 9:1 hexanes/ethyl acetate to afford **10e** as an orange solid (592 mg, 42%): ^{1}H NMR (500 MHz, $CDCl_3$) δ 5.18 (d, 4H, J = 11.0 Hz), 5.63 (d, 4H, J = 17.9 Hz), 6.57 (dd, 4H, J = 17.6, 10.9 Hz), 6.78 (d, 2H, J = 7.2 Hz), 7.09 (d, 8H, J = 7.2 Hz), 7.19−7.24 (m, 2H), 7.50 (d, 8H, J = 7.2 Hz), 7.57 (d, 2H, J = 8.3 Hz), 7.69 (s, 4H); ^{13}C NMR (100 MHz, $CDCl_3$) δ 114.3, 122.71, 124.57 (quartet, $^1J_{CF}$ = 272.4 Hz), 126.08, 126.41, 127.17, 127.64, 128.12 (quartet, $^2J_{CF}$ = 6.0 Hz), 129.06, 129.59, 130.42, 130.74, 136.45, 136.71, 138.1, 149.8, 160.1; HR-MS calcd for $[C_{58}H_{38}N_2F_6 + Na]^+$ 899.2837, found 899.2828.

General Procedure for Ring-Closing Metathesis (refs 12, 13). A solution of the open diimine in CH_2Cl_2 (0.001 M) was degassed under an a N_2 stream for 20 min and then heated to reflux. Grubbs second-generation catalyst (10 mol %) was added, and the mixture stirred until completed according to ES-MS. The solution was concentrated *in vacuo*, and the cyclophane ligand was purified accordingly.

NMe_2-Cyclophane, Unhydrogenated (11a). Following the general procedure for ring-closing methathesis, diimine **10a** (413 mg, 0.536 mmol) and Grubbs catalyst (60 mg) were reacted in 500 mL of degassed CH_2Cl_2 for 2 h, then concentrated *in vacuo*. The residue was then taken up into 20 mL of $CHCl_3$ and precipitated in 150 mL of diethyl ether. The mixture was left to stand overnight at −35 °C and filtered through Celite, and the solid was recovered in $CHCl_3$, then dried *in vacuo* to afford **11a** as a magenta solid (371 mg, 90%): ^{1}H NMR (500 MHz, $CDCl_3$) δ 3.05 (s, 12H), 6.48 (d, 4H, J = 7.7 Hz), 6.69 (d, 4H, J = 7.6 Hz), 6.82 − 6.89 (m, 14H), 7.36 (d, 4H, J = 7.7 Hz), 7.44 (t, 2H, J = 7.6 Hz), 7.85 (d, 2H, J = 8.3 Hz); ^{13}C NMR (125 MHz, $CDCl_3$) δ 41.4, 114.4, 123.6, 127.7, 128.51, 128.56, 128.86, 129.53, 129.83, 131.10, 131.24, 131.85, 133.2, 137.1, 138.5, 139.3, 140.2, 147.8, 162.9; HR-MS calcd for $[C_{56}H_{42}N_4 + H]^+$ 771.3488, found 771.3485.

OMe-Cyclophane, Unhydrogenated (11b). Following the general procedure for ring-closing methathesis, diimine **10b** (556 mg, 0.694 mmol) and Grubbs catalyst (60 mg) were reacted in 550 mL of degassed CH_2Cl_2 for 2 h, then concentrated *in vacuo*. The residue was washed in ethyl acetate (10 mL) and then diethyl ether (80 mL) and decanted. The solid was dried *in vacuo* to afford **11b** as a rust-colored solid (467 mg, 90%): ^{1}H NMR (500 MHz, $C_2D_2Cl_4$) δ 3.94 (s, 6H), 6.51 (d, 4H, J = 7.3 Hz), 6.69 (d, 4H, J = 7.4 Hz), 6.79−6.86 (m, 10H), 7.04 (s, 4H), 7.35 (d, 4H, J = 7.6 Hz), 7.46 (t, 2H, J = 7.6 Hz), 7.89 (d, 2H, J = 8.3 Hz); ^{13}C NMR (125 MHz, $CDCl_3$) δ 55.7, 115.0, 123.4, 127.77, 128.45, 128.74, 129.02, 129.39, 130.67, 131.01, 131.86, 132.95, 137.05, 137.34, 139.8, 141.6, 156.0, 162.6.

Cl-Cyclophane, Unhydrogenated (11d). Following the general procedure for ring-closing methathesis, diimine **10d** (451 mg, 0.557 mmol) and Grubbs catalyst (50 mg) were reacted in 500 mL of degassed CH_2Cl_2 for 2 h, then concentrated *in vacuo*. The residue was washed twice with 5 mL portions of ethyl acetate and then dried *in vacuo* to afford **11d** as a yellow-orange solid (365 mg, 87%): ^{1}H NMR (500 MHz, $CDCl_3$) δ 6.51 (d, 4H, J = 7.7 Hz), 6.68 (d, 4H, J = 7.5 Hz), 6.83−6.89 (m, 10H), 7.32 (d, 4H, J = 7.6 Hz), 7.44 (s, 4H), 7.52 (t, 2H, J = 7.7 Hz), 7.95 (d, 2H, J = 8.3 Hz); ^{13}C NMR (125 MHz, $CDCl_3$) δ 123.7, 127.5, 128.52, 129.04, 129.32, 129.36, 129.42, 129.66, 130.4, 131.2, 132.8, 133.1, 136.2, 137.6, 140.2, 146.5, 162.1; HR-MS calcd for $[C_{52}H_{30}Cl_2N_2 + H]^+$ 775.1684, found 775.1668.

CF_3-Cyclophane, Unhydrogenated (11e). Following the general procedure for ring-closing methathesis, diimine **10e** (250 mg, 0.285 mmol) and Grubbs catalyst (30 mg) were reacted in 250 mL of degassed toluene at 75 °C for 6 h. The mixture was passed through a plug of Celite and silica gel (on top) and then concentrated *in vacuo*. The solid was washed with 10 mL of methanol, then dried *in vacuo* to afford **11e** as a yellow solid (189 mg, 81%): ^{1}H NMR (500 MHz, $CDCl_3$) δ 6.56 (d, 4H, J = 7.6 Hz), 6.73 (d, 4H, J = 7.6 Hz), 6.83 (d, 2H, J = 7.2 Hz), 6.86−6.90 (m, 8H), 7.36 (d, 4H, J = 7.7 Hz), 7.52 (t, 2H, J = 7.8 Hz), 7.73 (s, 4H), 7.97 (d, 2H, J = 8.3 Hz); ^{13}C NMR (125 MHz, $CDCl_3$) δ 124.5 (quartet, $^1J_{CF}$ = 272.9 Hz), 123.8, 126.7 (quartet $^2J_{CF}$ = 3.2 Hz), 127.7, 128.78, 129.31, 129.40, 129.73, 129.91, 130.4, 131.40, 131.93, 133.3, 136.2, 137.9, 140.4, 150.8, 161.7; HR-MS calcd for $[C_{54}H_{30}N_2F_6 + H]^+$ 821.2391, found 821.2404.

NMe_2-Cyclophane, Hydrogenated (NMe_2-Cyc, 1a). Palladium on activated carbon (100 mg, 10 wt % Pd) was added to a N_2-degassed solution of diimine **11a** (371 mg, 0.481 mmol) in 120 mL of methanol, 200 mL of CH_2Cl_2, and 1.0 mL of triethylamine. The mixture was purged with hydrogen for 5 min, stirred under a hydrogen atmosphere for 90 min at room temperature, filtered through Celite, and

concentrated *in vacuo* to 20 mL. The mixture was decanted, and the solid was washed with 10 mL of methanol, decanted again, and dried overnight under high vacuum to afford **1a** as a magenta solid (352 mg, 94%): ^{1}H NMR (500 MHz, $C_2D_2Cl_4$) δ 2.76−3.02 (m, 8H), 3.00 (s, 12H), 6.36 (d, 4H, J = 7.7 Hz), 6.52 (d, 4H, J = 7.7 Hz), 6.78 (d, 4H, J = 7.9 Hz), 6.78 (s, 4H), 6.83 (d, 2H, J = 7.2 Hz), 7.27 (d, 4H, J = 7.9 Hz), 7.47 (t, 2H, J = 7.9 Hz), 7.87 (d, 2H, J = 8.2 Hz); ^{13}C NMR (125 MHz, $CDCl_3$) δ 35.7, 41.2, 99.4, 114.1, 123.0, 127.53, 127.88, 128.02, 128.12, 128.60, 129.06, 130.7, 131.4, 137.2, 138.2, 139.06, 139.61, 147.2, 161.7; HR-MS calcd for $[C_{56}H_{46}N_4 + H]^+$ 775.3801, found 775.3809.

OMe-Cyclophane, Hydrogenated (OMe-Cyc, 1b). Palladium on activated carbon (100 mg, 10 wt % Pd) was added to a N_2-degassed suspension of diimine **11b** (64 mg, 0.086 mmol) in 50 mL of methanol, 70 mL of CH_2Cl_2, and 5.0 mL of triethylamine. The diimine was poorly soluble. The mixture was purged with hydrogen for 5 min, stirred under a hydrogen atmosphere for 3 h at room temperature, filtered through Celite, and concentrated *in vacuo*. The solid was washed twice with 10 mL of methanol, then once with dichloromethane, and dried overnight under high vacuum to afford **1b** as an orange solid (352 mg, 33%). The product contained inseparable impurities: ^{1}H NMR (500 MHz, $C_2D_2Cl_4$) δ 2.73−3.00 (m, 8H), 3.09 (s, 12H), 6.37 (d, 4H, J = 7.5 Hz), 6.51 (d, 4H, J = 7.3 Hz), 6.72−6.80 (m, 6H), 6.94 (s, 4H), 7.27 (d, 2H, J = 7.2 Hz), 7.47 (d, 4H, J = 7.3 Hz), 7.89 (t, 2H, J = 7.8 Hz); ^{13}C NMR (125 MHz, $C_2D_2Cl_4$) δ 35.8, 55.6, 99.4, 114.49, 114.78, 123.0, 127.42, 128.01, 128.14, 128.70, 128.76, 128.99, 130.73, 130.90, 136.3, 138.5, 155.5, 161.5.

Cl-Cyclophane, Hydrogenated (Cl-Cyc, 1d). Palladium on activated carbon (50 mg, 10 wt % Pd) was added to a N_2-degassed solution of diimine **11d** (115 mg, 0.153 mmol) in 20 mL of methanol, 20 mL of CH_2Cl_2, and 1.0 mL of triethylamine. The mixture was purged with hydrogen for 5 min, stirred under a hydrogen atmosphere for 2 h at room temperature, filtered through Celite, and concentrated *in vacuo* to 5 mL. The mixture was decanted, and the solid was washed with 10 mL of methanol, decanted again, and dried overnight under high vacuum to afford **1d** as a yellow solid (76 mg, 66%): ^{1}H NMR (500 MHz, $C_2D_2Cl_4$) δ 2.75−2.96 (m, 8H), 6.37 (d, 4H, J = 7.7 Hz), 6.50 (d, 4H, J = 7.7 Hz), 6.77 (d, 4H, J = 7.7 Hz), 6.83 (d, 2H, J = 7.2 Hz), 7.24 (d, 4H, J = 7.8 Hz), 7.35 (s, 4H), 7.51 (t, 2H, J = 7.9 Hz), 7.93 (d, 2H, J = 8.3 Hz); ^{13}C NMR (125 MHz, $CDCl_3$) δ 35.9, 99.4, 123.1, 127.36, 128.18, 128.27, 128.35, 128.75, 128.81, 130.16, 130.82, 132.5, 135.1, 138.98, 139.81, 146.7, 160.7; HR-MS calcd for $[C_{52}H_{34}N_2Cl_2 + H]^+$ 757.2127, found 757.2203.

CF_3-Cyclophane, Hydrogenated (CF_3-Cyc, 1e). Palladium on activated carbon (20 mg, 10 wt % Pd) was added to a N_2-degassed solution of diimine **11e** (80 mg, 0.098 mmol) in 10 mL of methanol, 10 mL of CH_2Cl_2, and 1.0 mL of triethylamine. The mixture was purged with hydrogen for 5 min, stirred under a hydrogen atmosphere for 1 h at room temperature, filtered through Celite, and concentrated *in vacuo*. The residue was washed with 10 mL of methanol and dried overnight under high vacuum to afford **1e** as a yellow solid (44 mg, 55%): ^{1}H NMR (500 MHz, $CDCl_3$) δ 2.79−3.00 (m, 8H), 6.40 (d, 4H, J = 7.7 Hz), 6.58 (d, 4H, J = 7.6 Hz), 6.75 (d, 2H, J = 7.2 Hz), 6.82 (d, 4H, J = 8.0 Hz), 7.28 (d, 4H, J = 7.7 Hz), 7.52 (t, 2H, J = 7.8 Hz), 7.60 (s, 4H), 7.95 (d, 2H, J = 8.3 Hz); ^{13}C NMR (125 MHz, $CDCl_3$) δ 36.1, 123.63, 124.64 (quartet, $^1J_{CF}$ = 272.3 Hz), 126.11, 126.38 (quartet $^2J_{CF}$ = 3.7 Hz), 127.63, 128.48, 128.65, 129.32, 129.36, 129.42, 130.52, 131.31, 132.13, 135.5, 139.5, 140.5, 151.4, 160.4; HR-MS calcd for $[C_{54}H_{34}N_2F_6 + Na]^+$ 847.2524, found 847.2511.

Spectral Data for $B(C_6F_5)_4^-$ Anion. ^{13}C NMR (125 MHz, $CDCl_3$) δ 135.9, 137.8, 139.7, 147.7, 149.6. All signals are broadened by splitting. ^{19}F NMR (376 MHz, $CDCl_3$) δ −167.12 (m, 8F), −163.53 (t, 4F, J_{FF} = 20.4 Hz), −132.73 (s, 8F).

[(NMe_2-Cyc)Ni(acac)]$B(C_6F_5)_4$ (2a). A scintillation vial was charged with diimine **1a** (33 mg, 0.043 mmol), trityl tetrakis(pentafluorophenyl)borate (39 mg, 0.043 mmol), and $Ni(acac)_2$ (11 mg, 0.043 mmol). To this was added 10 mL of dry CH_2Cl_2, and the reaction was stirred for 1 h at room temperature. The mixture was concentrated *in vacuo* to 2 mL, and dry diethyl ether (2 mL) and pentane (15 mL) were added. The mixture was decanted, and the solid washed with 10 mL of diethyl ether and 10 mL of pentane, then dried for two days *in vacuo* to afford **2a** as a deep violet solid (51 mg, 74%): ^{1}H NMR (500 MHz, $CDCl_3$) δ 1.83 (s, 6H), 2.98 (s, 12 H), 3.05−3.21 (m, 8H), 5.50 (s, 1H), 6.42 (d, 4H, J = 7.9 Hz), 6.54 (s, 4H), 6.59 (d, 4H, J = 7.9 Hz), 6.94 (d, 2H, J = 7.1 Hz), 7.21 (d, 4H, J = 7.8 Hz), 7.27 (d, 4H, J = 7.7 Hz), 7.66 (t, 2H, J = 8.0 Hz), 8.15 (d, 2H, J = 8.3 Hz); ^{13}C NMR (125 MHz, CD_2Cl_2) δ 25.2, 35.1, 40.7, 102.5, 113.8, 125.90, 126.44, 127.60,127.88, 128.89, 129.41, 130.15, 130.58, 132.13, 132.96, 136.8, 138.0, 140.4, 147.7, 150.1, 173.9, 187.8. Anal. Calcd for $C_{85}H_{53}N_4O_2BF_{20}Ni$ + 0.22 CH_2Cl_2: C, 62.77; H, 3.30; N, 3.44. Found: C, 62.54; H, 3.27; N, 3.48.

[(OMe-Cyc)Ni(acac)]$B(C_6F_5)_4$ (2b). A scintillation vial was charged with diimine **1b** (33 mg, 0.044 mmol), trityl tetrakis(pentafluorophenyl)-borate (41 mg, 0.044 mmol), and $Ni(acac)_2$ (11 mg, 0.043 mmol). To this was added 5 mL of dry CH_2Cl_2, and the reaction was stirred overnight at room temperature. The mixture was concentrated *in vacuo* to 2 mL, and dry diethyl ether (4 mL) and pentane (15 mL) were added. The mixture was decanted, and the solid washed with 8 mL of diethyl ether and 12 mL of pentane, then dried for two days *in vacuo* to afford **2b** as a red-brown solid (51 mg, 73%): ^{1}H NMR (600 MHz, $CDCl_3$) δ 1.82 (s, 6H), 3.03−3.24 (m, 8H), 3.86 (s, 6H), 5.54 (s, 1H), 6.42 (d, 4H, J = 7.1 Hz), 6.61 (d, 4H, J = 7.1 Hz), 6.82 (s, 4H), 6.90 (d, 2H, J = 7.2 Hz), 7.23 (d, 4H, J = 7.3 Hz), 7.27 (d, 4H, J = 7.7 Hz), 7.68 (t, 2H, J = 7.6 Hz), 8.19 (d, 2H, J = 8.1 Hz); ^{13}C NMR (125 MHz, $CDCl_3$) δ 25.1, 34.8, 55.9, 102.6, 116.0, 125.0, 126.22, 127.06, 128.22, 129.43, 129.88, 130.49, 130.99, 133.5, 135.2, 137.36, 138.27, 140.5, 159.0, 173.6, 187.4. Anal. Calcd for $C_{83}H_{47}N_2O_4BF_{20}Ni$: C, 62.87; H, 2.99; N, 1.77. Found: C, 61.65; H, 2.93; N, 1.78.

[(Me-Cyc)Ni(acac)]$B(C_6F_5)_4$ (2c). A scintillation vial was charged with diimine **1c** (54 mg, 0.075 mmol), trityl tetrakis(pentafluorophenyl)borate (70 mg, 0.075 mmol), and $Ni(acac)_2$ (19 mg, 0.075 mmol). To this were added 2 mL of dry CH_2Cl_2 and 8 mL of dry diethyl ether, and the reaction was stirred for 1 h at room temperature. Pentane (10 mL) was added, the mixture was decanted, and the solid was washed with 10 mL of diethyl ether and 10 mL of pentane. The solid was dried for two days *in vacuo* to afford **2c** as a dark red solid (72 mg, 93%): ^{1}H NMR (500 MHz, CD_2Cl_2) δ 1.79 (s, 6H), 2.38 (s, 6 H), 3.03−3.22 (m, 8H), 5.56 (s, 1H), 6.44 (d, 4H, J = 7.8 Hz), 6.60 (d, 4H, J = 7.8 Hz), 6.85 (d, 2H, J = 7.2 Hz), 7.11 (s, 4H), 7.24 (d, 4H, J = 7.8 Hz), 7.30 (d, 4H, J = 7.8 Hz), 7.67 (t, 2H, J = 8.2 Hz), 8.22 (d, 2H, J = 8.0 Hz); ^{13}C NMR (125 MHz, CD_2Cl_2) δ 21.5, 25.1, 35.2, 102.7, 125.4, 126.84, 127.58, 128.84, 129.68, 130.29, 130.81, 131.83, 132.20, 133.63, 135.85, 135.97, 137.0, 139.3, 140.8, 173.7, 187.8. Anal. Calcd for $C_{83}H_{47}N_2O_2BF_{20}Ni$: C, 64.16; H, 3.05; N, 1.80. Found: C, 64.38; H, 3.08; N, 1.74.

[(Cl-Cyc)Ni(acac)]$B(C_6F_5)_4$ (2d). A scintillation vial was charged with diimine **1d** (43 mg, 0.057 mmol), trityl tetrakis(pentafluorophenyl)borate (52 mg, 0.057 mmol), and $Ni(acac)_2$ (15 mg, 0.057 mmol). To this was added 7 mL of dry CH_2Cl_2, and the reaction was stirred for 1 h at room temperature. Diethyl ether (12 mL) was added, and a light-colored precipitate resulted. The mixture was decanted, and the supernatant was concentrated *in vacuo* to 5 mL. Pentane (15 mL) was added, the mixture was decanted, and the solid was dried for two days *in vacuo* to afford **2d** as a dark red solid (34 mg, 38%): ^{1}H NMR (500 MHz, $CDCl_3$) δ 1.82 (s, 6H), 3.04−3.23 (m, 8H), 5.55 (s, 1H), 6.40 (d, 4H, J = 7.8 Hz), 6.61 (d, 4H, J = 7.8 Hz), 6.93 (d, 2H, J = 7.2 Hz), 7.23 (s, 8H), 7.31 (s, 4H), 7.72 (t, 2H, J = 7.9 Hz), 8.21 (d, 2H, J = 8.4 Hz); ^{13}C NMR (125 MHz, CD_2Cl_2) δ 25.3, 35.1, 103.0, 125.0, 127.05, 127.40, 128.6, 129.91, 130.56, 131.01, 131.12, 132.31, 134.28, 134.31, 134.42, 136.9, 139.0, 141.5, 173.8, 187.9. Anal. Calcd for $C_{81}H_{41}N_2O_2Cl_2BF_{20}Ni$: C, 61.01; H, 2.59; N, 1.76. Found: C, 61.24; H, 2.63; N, 1.84.

[(CF$_3$-Cyc)Ni(acac)]B(C$_6$F$_5$)$_4$ (2e). A scintillation vial was charged with diimine **1e** (36 mg, 0.044 mmol), trityl tetrakis(pentafluorophenyl)-borate (41 mg, 0.044 mmol), and Ni(acac)$_2$ (11 mg, 0.044 mmol). To this was added 4 mL of dry CH_2Cl_2, and the reaction was stirred for 1 h at room temperature. Diethyl ether (4 mL) and 10 mL of pentane were added, and the mixture was decanted. The solid was washed with 5 mL of diethyl ether, then 5 mL of pentane, and dried for two days *in vacuo* to afford **2e** as a dark red solid (50 mg, 68%): ^{1}H NMR (600 MHz, $CDCl_3$) δ 1.78 (s, 6H), 3.05−3.26 (m, 8H), 5.57 (s, 1H), 6.46 (d, 4H, J = 7.6 Hz), 6.65 (d, 4H, J = 7.8 Hz), 6.89 (d, 2H, J = 7.2 Hz), 7.24 (d, 4H, J = 8.1 Hz), 7.29 (d, 4H, J = 7.8 Hz), 7.59 (s, 4H), 7.73 (t, 2H, J = 7.8 Hz), 8.25 (d, 2H, J = 8.5 Hz); ^{13}C NMR (125 MHz, $C_2D_2Cl_4$) δ 24.5, 34.4, 102.6, 123.2 (d, $^1J_{CF}$ = 273.3 Hz), 126.09, 126.67, 127.28, 127.80, 129.47, 130.01, 130.56, 131.56, 133.21, 134.21, 137.81, 140.34, 141.02, 148.2, 172.6, 187.0. Anal. Calcd for $C_{83}H_{41}N_2O_2BF_{26}Ni$: C, 59.99; H, 2.49; N, 1.69. Found: C, 59.69; H, 2.46; N, 1.68.

[(Acyc)Ni(acac)]B(C$_6$F$_5$)$_4$ (12). A scintillation vial was charged with *N*,*N*′-bis(2,6-diisopropyl)phenylacenaphthenequinonediimine (50 mg, 0.10 mmol), trityl tetrakis(pentafluorophenyl)borate (92 mg, 0.10 mmol), and Ni(acac)$_2$ (26 mg, 0.10 mmol). To this was added 10 mL of dry diethyl ether, and the reaction was stirred for 1 h at room temperature. The mixture was concentrated *in vacuo* to 2 mL, and dry diethyl ether (5 mL) and pentane (10 mL) were added. The residue was redissolved in 5 mL of diethyl ether, precipitated with 10 mL of pentane, decanted, and then dried for two days *in vacuo* to afford **12** as a dark red solid (121 mg, 91%): ^{1}H NMR (500 MHz, $CDCl_3$) δ 1.11 (d, 12H, J = 6.9 Hz), 1.55 (d, 12H, J = 6.9 Hz), 1.57 (s, 6H), 3.70 (septet, 4H, J = 6.9 Hz), 5.48 (s, 1H), 6.80 (d, 2H, J = 7.2 Hz), 7.37 (d, 4H, J = 7.8 Hz), 7.57 (t, 4H, J = 7.7 Hz), 8.18 (d, 2H, J = 8.3 Hz); ^{13}C NMR (125 MHz, CD_2Cl_2) δ 23.71, 23.82, 24.6, 30.3, 102.6, 123.8, 124.74, 126.4, 129.77, 130.17, 131.88, 134.1, 137.3, 141.0, 149.0, 173.4, 187.9. Anal. Calcd for $C_{65}H_{47}N_2O_2BF_{20}Ni$: C, 58.37; H, 3.54; N, 2.09. Found: C, 58.25; H, 3.45; N, 2.15.

(OMe-Cyc)PdMeCl, Unhydrogenated (14b). Tetramethyltin (0.155 mL, 204 mg, 1.14 mmol, 3.4 equiv) was added to a solution of dichlorobis(benzonitrile)palladium(II) (167 mg, 0.436 mmol, 1.3 equiv) in 20 mL of dry CH_2Cl_2 at −35 °C. The reaction was maintained at this temperature for 2.5 h with stirring, after which was added a suspension of diimine **11b** (250 mg, 0.336 mmol, 1.0 equiv) in 20 mL of dry CH_2Cl_2. The mixture was warmed to room temperature and stirred overnight, filtered through Celite, and then concentrated *in vacuo* to 5 mL. Diethyl ether (30 mL) was added, and the mixture was allowed to stand for 4 h, then decanted. The residue was rinsed with 20 mL of diethyl ether, decanted, and dried *in vacuo* to afford **14b** as a red-brown solid (260 mg, 86%): ^{1}H NMR (500 MHz, $CDCl_3$) δ 0.66 (s, 3H), 3.90 (s, 3H), 3.93 (s, 3H), 6.12 (d, 2H, J = 8.2 Hz), 6.29 (d, 2H, J = 8.1 Hz), 6.42 (d, 1H, J = 7.2 Hz), 6.79−6.83 (m, 4H), 6.86 (d, 2H, J = 8.0 Hz), 6.94 (s, 4H), 6.95 (s, 2H), 7.01 (s, 2H), 7.14 (d, 1H, J = 7.2 Hz), 7.32 (d, 2H, J = 8.1 Hz), 7.38 (d, 2H, J = 8.0 Hz), 7.55 (t, 1H, J = 7.7 Hz), 7.57 (t, 1H, J = 7.7 Hz), 8.06 (d, 1H, J = 8.2 Hz), 8.09 (d, 1H, J = 8.2 Hz), 8.68 (d, 2H, J = 8.1 Hz); ^{13}C NMR (125 MHz, $CDCl_3$) δ 2.5, 55.79, 55.89, 115.43, 115.88, 124.4, 125.3, 126.94, 127.21, 127.36, 127.77, 129.11, 129.16, 129.34, 129.51, 129.56, 130.14, 130.74, 131.25, 131.51, 131.66, 131.68, 133.36, 134.48, 135.00, 135.99, 136.01, 136.26, 136.42, 137.30, 137.73, 138.7, 143.2, 157.9, 158.4, 167.8, 173.8; HR-MS calcd for $[C_{55}H_{39}ClN_2O_2Pd - Cl^- + CH_3CN]^+$ 906.2332, found 906.2342.

(Cl-Cyc)PdMeCl, Unhydrogenated (14d). Tetramethyltin (0.154 mL, 202 mg, 1.13 mmol, 3.4 equiv) was added to a solution of dichlorobis(benzonitrile)palladium(II) (165 mg, 0.431 mmol, 1.3 equiv) in 20 mL of dry CH_2Cl_2 at −35 °C. The reaction was maintained at this temperature for 2.5 h with stirring, after which was added a suspension of diimine **11d** (250 mg, 0.332 mmol, 1.0 equiv) in 20 mL of dry CH_2Cl_2. The mixture was warmed to room temperature and stirred overnight, concentrated *in vacuo*, and then purified by flash chromatography in 2% ethyl acetate in CH_2Cl_2. The red fractions were collected, concentrated *in vacuo*, rinsed with diethyl ether (10 mL), then dried *in vacuo* to afford **14d** as a red-brown solid (246 mg, 81%): ^{1}H NMR (500 MHz, $CDCl_3$) δ 0.66 (s, 3H), 6.12 (d, 2H, J = 8.2 Hz), 6.26 (d, 2H, J = 8.2 Hz), 6.45 (d, 1H, J = 7.2 Hz), 6.79 (d, 4H, J = 7.9 Hz), 6.87 (d, 2H, J = 7.9 Hz), 6.95 (s, 4H), 7.15 (d, 1H, J = 7.2 Hz), 7.32 − 7.37 (m, 4H), 7.39 (s, 2H), 7.49 (s, 2H), 7.60 (t, 1H, J = 7.7 Hz), 7.62 (t, 1H, J = 7.7 Hz), 8.11 (d, 1H, J = 8.2 Hz), 8.15 (d, 1H, J = 8.2 Hz), 8.65 (d, 2H, J = 8.2 Hz); ^{13}C NMR (125 MHz, $CDCl_3$) δ 2.7, 124.5, 125.4, 126.97, 127.00, 127.13, 128.01, 128.96, 129.09, 129.38, 129.72, 129.92, 130.33, 130.63, 131.31, 131.42, 131.62, 131.79, 132.81, 132.83, 133.40, 134.52, 134.92, 135.14, 136.50, 136.59, 138.1, 139.1, 140.0, 142.4, 143.4, 167.2, 173.5; HR-MS calcd for $[C_{53}H_{33}Cl_3N_2Pd - Cl^- + CH_3CN]^+$ 916.1324, found 916.1304.

(CF$_3$-Cyc)PdMeCl, Unhydrogenated (14e). Tetramethyltin (0.066 mL, 87 mg, 0.49 mmol, 3.4 equiv) was added to a solution of dichlorobis(benzonitrile)palladium(II) (71 mg, 0.19 mmol, 1.3 equiv) in 10 mL of dry CH_2Cl_2 at −35 °C. The reaction was maintained at this temperature for 2.5 h with stirring, after which was added a suspension of diimine **11e** (117 mg, 0.143 mmol, 1.0 equiv) in 10 mL of dry CH_2Cl_2. The mixture was warmed to room temperature and stirred overnight, concentrated *in vacuo*, and then purified by flash chromatography in CH_2Cl_2. The red fractions were collected, then dried *in vacuo* overnight to afford **14e** as a red-brown solid (96 mg, 69%): ^{1}H NMR (500 MHz, $CDCl_3$) δ 0.66 (s, 3H), 6.16 (d, 2H, J = 8.2 Hz), 6.30 (d, 2H, J = 8.1 Hz), 6.34 (d, 1H, J = 7.3 Hz), 6.81−6.85 (m, 4H), 6.90 (d, 2H, J = 7.7 Hz), 6.97 (s, 4H), 7.06 (d, 1H, J = 7.3 Hz), 7.35−7.40 (m, 4H), 7.60 (t, 2H, J = 7.3 Hz), 7.66 (s, 2H), 7.76 (s, 2H), 8.14 (d, 1H, J = 8.4 Hz), 8.18 (d, 1H, J = 8.2 Hz), 8.66 (d, 2H, J = 8.2 Hz); ^{13}C NMR (125 MHz, $CDCl_3$) δ 2.8, 123.75 (quartet, $^1J_{CF}$ = 264.2 Hz), 124.01 (quartet, $^1J_{CF}$ = 273.0 Hz), 124.44, 125.44, 126.90, 127.09, 127.14, 127.81, 128.18, 128.80, 129.17, 129.55, 129.82, 129.92, 130.43, 131.34, 131.55, 131.70, 131.87, 132.07, 133.45, 134.58, 134.76, 135.04, 135.87, 135.90, 138.4, 139.4, 143.5, 144.2, 146.7, 166.7, 173.3; HR-MS calcd for $[C_{55}H_{33}ClF_6N_2Pd - Cl^- + CH_3CN]^+$ 982.1868, found 982.1841.

(NMe$_2$-Cyc)PdMeCl, Hydrogenated (3a). Tetramethyltin (0.138 mL, 182 mg, 1.02 mmol, 3.4 equiv) was added to a solution of dichlorobis(benzonitrile)palladium(II) (149 mg, 0.389 mmol, 1.3 equiv) in 20 mL of dry CH_2Cl_2 at −35 °C. The reaction was maintained at this temperature for 2.5 h with stirring, after which was added a suspension of diimine **1a** (232 mg, 0.299 mmol, 1.0 equiv) in 20 mL of dry CH_2Cl_2. The mixture was warmed to room temperature and stirred overnight. The mixture was concentrated *in vacuo* to 20 mL, 150 mL of diethyl ether was added, and the mixture was stored overnight at −35 °C. The mixture was decanted, and the solid was dried *in vacuo* for 24 h to afford **3a** as an olive green solid (233 mg, 84%): ^{1}H NMR (600 MHz, $CDCl_3$) δ 0.78 (s, 3H), 2.75−3.20 (m, 8H), 2.97 (s, 6H), 3.01 (s, 6H), 6.14 (d, 2H, J = 7.5 Hz), 6.24 (d, 2H, J = 7.6 Hz), 6.45 (d, 1H, J = 7.1 Hz), 6.57 (d, 2H, J = 7.5 Hz), 6.65 (s, 2H), 6.66 (s, 2H), 6.71 (d, 2H, J = 7.6 Hz), 6.92 (d, 2H, J = 7.5 Hz), 7.12 (d, 1H, J = 7.1 Hz), 7.2 (d, 2H, J = 7.5 Hz), 7.34 (d, 2H, J = 7.6 Hz), 7.54 (t, 2H, J = 7.6 Hz), 8.02 (d, 1H, J = 8.3 Hz), 8.06 (d, 1H, J = 8.3 Hz), 8.38 (d, 2H, J = 7.6 Hz); ^{13}C NMR (125 MHz, $CDCl_3$) δ 2.2, 34.44, 34.67, 40.56, 113.3, 124.18, 124.89, 126.77, 127.22, 127.57, 128.51, 128.68, 128.75, 129.24, 129.39, 129.95, 130.41, 130.52, 131.16, 131.47, 135.39, 135.64, 136.06, 138.60, 139.23, 143.0, 148.4, 167.7, 172.2. Anal. Calcd for $C_{57}H_{49}N_4ClPd$ + 0.11 CH_2Cl_2: C, 72.88; H, 5.27; N, 5.95. Found: C, 72.46; H, 5.20; N, 5.97.

(OMe-Cyc)PdMeCl, Hydrogenated (3b). Palladium on activated carbon (100 mg, 10 wt % Pd) was added to a N_2-degassed solution of complex **14b** (260 mg, 0.288 mmol) in 200 mL of methanol and 200 mL of CH_2Cl_2. The mixture was purged with hydrogen for 5 min,

stirred under a hydrogen atmosphere for 3 h at room temperature, filtered through Celite, and then concentrated *in vacuo* to 20 mL. The mixture was filtered, and the solid was washed with methanol and dried overnight *in vacuo* to afford **14b** as a red-brown solid (245 mg, 94%): ^{1}H NMR (500 MHz, $CDCl_3$) δ 0.76 (s, 3H), 2.75−3.21 (m, 8H), 3.86 (s, 3H), 3.88 (s, 3H), 6.12 (d, 2H, J = 7.9 Hz), 6.21 (d, 2H, J = 7.9 Hz), 6.35 (d, 1H, J = 7.2 Hz), 6.56 (d, 2H, J = 7.7 Hz), 6.73 (d, 2H, J = 7.7 Hz), 6.86 (s, 2H), 6.90 (d, 2H, J = 7.7 Hz), 6.91 (s, 2H), 7.01 (s, 2H), 7.08 (d, 1H, J = 7.2 Hz), 7.27−7.33 (m, 4H), 7.56 (t, 1H, J = 7.8 Hz), 7.57 (t, 1H, J = 7.8 Hz), 8.05 (d, 1H, J = 8.3 Hz), 8.09 (d, 1H, J = 8.2 Hz), 8.40 (d, 2H, J = 8.0 Hz); ^{13}C NMR (125 MHz, $CDCl_3$) δ 2.2, 34.54, 34.77, 55.59, 55.69, 115.20, 115.59, 124.20, 124.93, 126.69, 127.07, 127.34, 128.66, 128.73, 129.23, 129.36, 130.27, 130.62, 130.74, 131.24, 131.39, 135.11, 135.38, 135.63, 136.01, 136.06, 137.4, 138.89, 139.58, 143.1, 157.49, 157.73, 167.4, 172.1. Anal. Calcd for $C_{55}H_{43}N_2O_2ClPd$: C, 72.39; H, 4.76; N, 3.06. Found: C, 72.10; H, 4.86; N, 3.08.

(Cl-Cyc)PdMeCl, Hydrogenated (3d). Palladium on activated carbon (50 mg, 10 wt % Pd) was added to a N_2-degassed solution of complex **14d** (246 mg, 0.270 mmol) in 100 mL of methanol and 100 mL of CH_2Cl_2. The mixture was purged with hydrogen for 5 min, stirred under a hydrogen atmosphere for 1 h at room temperature, filtered through Celite, and then concentrated *in vacuo*. The residue was washed with 10 mL of pentane and dried overnight under high vacuum to afford **3d** as a red-brown solid (222 mg, 90%): ^{1}H NMR (500 MHz, $CDCl_3$) δ 0.75 (s, 3H), 2.74−3.22 (m, 8H), 6.12 (d, 2H, J = 8.2 Hz), 6.20 (d, 2H, J = 8.2 Hz), 6.39 (d, 1H, J = 7.2 Hz), 6.55 (d, 4H, J = 7.8 Hz), 6.74 (d, 2H, J = 7.6 Hz), 6.87 (d, 2H, J = 6.9 Hz), 7.12 (d, 1H, J = 7.2 Hz), 7.29 (s, 4H), 7.30 (s, 2H), 7.38 (s, 2H), 7.62 (t, 2H, J = 7.2 Hz), 8.10 (d, 1H, J = 8.3 Hz), 8.15 (d, 1H, J = 8.2 Hz), 8.37 (d, 2H, J = 8.0 Hz); ^{13}C NMR (125 MHz, $CDCl_3$) δ 2.5, 34.59, 34.82, 124.3, 125.1, 126.67, 126.99, 127.55, 128.61, 128.85, 129.00, 129.45, 129.56, 129.69, 130.34, 130.72, 131.20, 131.38, 131.95, 132.2, 133.78, 134.10, 136.60, 136.64, 139.36, 140.09, 140.67, 142.5, 143.3, 166.7, 171.7. Anal. Calcd for $C_{53}H_{37}N_2Cl_3Pd + 0.13\ Et_2O + 0.14\ CH_2Cl_2$: C, 68.84; H, 4.15; N, 2.99. Found: C, 68.61; H, 4.18; N, 3.00.

(CF_3-Cyc)PdMeCl, Hydrogenated (3e). Palladium on activated carbon (25 mg, 10 wt % Pd) was added to a N_2-degassed solution of complex **14e** (65 mg, 0.066 mmol) in 20 mL of methanol and 20 mL of CH_2Cl_2. The mixture was purged with hydrogen for 5 min, stirred under a hydrogen atmosphere for 2 h at room temperature, filtered through Celite, and then concentrated *in vacuo* to 2 mL. The residue was washed twice with 10 mL of pentane and dried overnight under high vacuum to afford **3e** as a red-brown solid (50 mg, 77%): ^{1}H NMR (500 MHz, $CDCl_3$) δ 0.73 (s, 3H), 2.75−3.25 (m, 8H), 6.15 (d, 2H, J = 7.8 Hz), 6.23 (d, 2H, J = 8.1 Hz), 6.26 (d, 1H, J = 7.3 Hz), 6.59 (d, 2H, J = 7.7 Hz), 6.78 (d, 2H, J = 7.6 Hz), 6.89 (d, 2H, J = 8.0 Hz), 7.05 (d, 1H, J = 7.3 Hz), 7.28−7.33 (m, 4H), 7.57 (s, 2H), 7.57−7.66 (m, 2H), 7.66 (s, 2H), 8.13 (d, 1H, J = 8.3 Hz), 8.18 (d, 1H, J = 8.3 Hz), 8.38 (d, 2H, J = 8.2 Hz); ^{13}C NMR (125 MHz, $CDCl_3$) δ 2.7, 34.75, 34.97, 123.83 (quartet, $^1J_{CF}$ = 272.8 Hz), 124.07 (quartet, $^1J_{CF}$ = 272.3 Hz), 124.38, 125.3, 126.89, 126.98 (quartet, $^3J_{CF}$ = 4.6 Hz), 127.16, 127.66 (quartet, $^3J_{CF}$ = 3.7 Hz), 127.84, 128.82, 128.99, 129.13, 129.28, 129.67, 129.83, 130.94, 131.25, 131.31, 131.58, 131.72, 133.76, 134.11, 136.07, 136.10, 139.8, 140.5, 143.6, 145.0, 146.9, 166.4, 171.7. Anal. Calcd for $C_{55}H_{37}N_2ClF_6Pd$: C, 67.29; H, 3.80; N, 2.85. Found: C, 67.00; H, 3.70; N, 2.84.

Structural Assignment of (Me-Cyc)PdMeCl (3c), [(Me-Cyc)PdMe(NCMe)]BAF (18), and [(Me-Cyc)PdMe(Me_2S)]BAF (19). Assignments for the following three compounds were corroborated by COSY, HMQC, HMBC, and NOE experiments (see Supporting Information). The key NOE enhancements that aided assignment are shown as arrows in Figure 7. Proton assignments are given in capital letters (except methyl groups), and carbon assignments are given in lowercase letters.

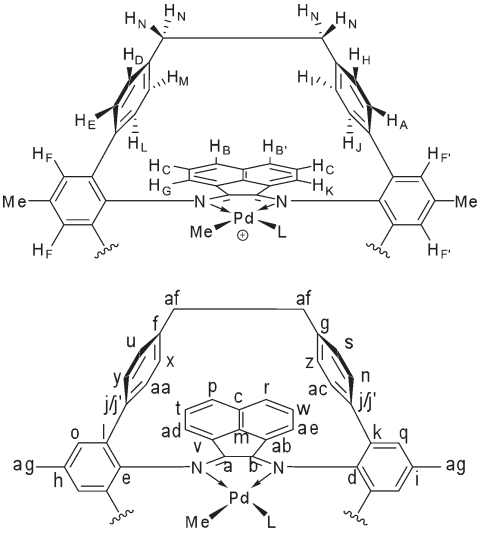

3c: L = Cl^-
18: L = MeCN
19: L = Me_2S

(Me-Cyc)PdMeCl (3c). The synthesis of complex **3c** is described elsewhere, along with NMR characterization without assignment.[12] Representative 2D NMR spectra and NOE measurements used during assignment are given in the Supporting Information. ^{1}H NMR (500 MHz, CD_2Cl_2) δ 0.58 (s, 3H, Pd-*Me*), 2.45 (s, 6H, Ar-*Me*), 2.70−3.21 (m, 8H, N), 6.05 (d, 2H, J = 7.8 Hz, M), 6.22 (d, 3H, J = 7.3 Hz, K/L), 6.60 (d, 2H, J = 7.6 Hz, J), 6.76 (d, 2H, J = 7.8 Hz, I), 6.80 (d, 2H, J = 7.7 Hz, H), 7.07 (d, 1H, J = 7.1 Hz, G), 7.11 (s, 2H, F′), 7.18 (s, 2H, F), 7.26 (d, 2H, J = 7.9 Hz, E), 7.31 (d, 2H, J = 7.9 Hz, D), 7.52 (t, 2H, J = 8.1 Hz, C), 8.04 (d, 1H, J = 8.3 Hz, B′), 8.09 (d, 1H, J = 8.3 Hz, B), 8.35 (d, 2H, J = 8.0 Hz, A); ^{13}C NMR (125 MHz, CD_2Cl_2) δ 1.6 (Pd-*Me*), 21.32 (Ar-*Me*), 21.34 (Ar-*Me*), 35.01 (af), 35.32 (af), 124.78 (ae), 125.79 (ad), 127.41 (ac), 127.63 (v/ab), 127.83 (aa), 127.96 (z), 129.09 (y), 129.13 (x), 129.33 (t/w), 129.60 (v/ab), 129.66 (u), 129.74 (t/w), 130.75 (s), 130.82 (r), 130.86 (q), 131.34 (p), 131.49 (o), 131.65 (n), 131.78 (m), 135.02 (l), 135.26 (k), 135.85 (j′), 135.86 (j), 137.04 (h/i), 137.15 (h/i), 139.49 (g), 140.01 (f), 140.14 (e), 142.13 (d), 143.7 (c), 167.5 (b), 172.4 (a).

[(Me-Cyc)PdMe(NCMe)]BAF (18). An oven-dried flask was charged with 26 mg of **3c** (0.030 mmol) and 27 mg of NaBAF (0.030 mmol). To this were added 5 mL of CH_2Cl_2 and 1.0 mL of acetonitrile, and the mixture was stirred overnight at room temperature. The mixture was filtered through Celite and concentrated *in vacuo* to ca. 1 mL. Pentanes (15 mL) were added, the mixture was left to stand for 30 min, and the supernatant was decanted. The solid residue was dried for 24 h *in vacuo* to afford **18** as a rust-colored solid (46 mg, 88%). Representative 2D NMR spectra and NOE measurements used during assignment are given in the Supporting Information. ^{1}H NMR (500 MHz, CD_2Cl_2) δ 0.72 (s, 3H, Pd-*Me*), 2.20 (s, 3H, NC*Me*), 2.45 (s, 3H, Ar-*Me*), 2.46 (s, 3H, Ar-*Me*), 2.81−3.22 (m, 8H, N), 6.23 (m, 4H, L/M), 6.50 (d, 1H, J = 7.2 Hz, K), 6.59 (d, 2H, J = 7.8 Hz, J), 6.75 (d, 2H, J = 7.9 Hz, I), 6.89 (d, 2H, J = 7.9 Hz, H), 6.97 (d, 2H, J = 7.2 Hz, G), 7.16 (d, 1H, J = 8.0 Hz, E), 7.17 (s, 2H, F), 7.19 (s, 2H, F), 7.21 (d, 2H, J = 7.8 Hz, D), 7.26 (d, 2H, J = 7.9 Hz, A), 7.57−7.62 (m, 2H, C), 8.12 (d, 1H, J = 8.3 Hz, B′), 8.15 (d, 1H, J = 8.3 Hz, B); ^{13}C NMR (125 MHz, CD_2Cl_2) δ 3.9 (NC*Me*), 7.0 (Pd-*Me*), 21.27 (Ar-*Me*), 21.33 (Ar-*Me*), 34.95 (af), 35.01 (af), 121.79 (NCMe), 125.70 (ae), 126.52 (ab), 126.90 (ad), 127.80 (aa),

dx.doi.org/10.1021/om200193r |*Organometallics* 2011, 30, 2432–2452

127.91 (v/ac), 128.66 (y), 128.96 (n), 129.37 (z), 129.56 (x), 129.76 (t), 129.83 (u), 130.01 (w), 130.49 (s), 131.46 (o), 131.88 (m), 131.94 (q), 132.30 (p), 133.09 (r), 135.03 (j/j′), 135.26 (l), 135.42 (k), 138.05 (h), 138.68 (i), 138.81 (d), 140.37 (f/g), 140.41 (f/g), 140.75 (e), 145.25 (c), 169.7 (b), 176.3 (a). Anal. Calcd for $C_{89}H_{58}N_3PdBF_{24}$: C, 61.34; H, 3.35; N, 2.41. Found: C, 61.64; H, 3.32; N, 2.39.

[(Me-Cyc)PdMe(Me$_2$S)]BAF (19). Complex **19** was prepared *in situ* by the addition of 1 equiv of dimethyl sulfide to a CD_2Cl_2 solution of **18**. Representative 2D NMR spectra and NOE measurements used during assignment are given in the Supporting Information. ^{1}H NMR (500 MHz, CD_2Cl_2) δ 0.69 (s, 3H, Pd-*Me*), 2.20 (s, 6H, S*Me*$_2$), 2.45 (s, 3H, Ar-*Me*), 2.46 (s, 3H, Ar-*Me*), 2.93 − 3.09 (m, 8H, N), 6.38 (d, 2H, J = 7.8 Hz, L), 6.40 (d, 2H, J = 7.8 Hz, J), 6.50 (d, 2H, J = 8.0 Hz, I), 6.52 (d, 2H, J = 7.9 Hz, M), 6.82 (d, 1H, J = 7.4 Hz, G), 6.90 (d, 1H, J = 7.2 Hz, K), 6.92 (d, 2H, J = 8.0 Hz, D), 6.97 (d, 2H, J = 7.9 Hz, H), 7.05 (d, 2H, J = 7.6 Hz, A), 7.15 (d, 2H, J = 7.9 Hz, E), 7.19 (s, 2H, F/F′), 7.21 (s, 2H, F/F′), 7.63 (t, 1H, J = 8.1 Hz, C), 7.65 (t, 1H, J = 8.1 Hz, C), 8.16 (d, 1H, J = 8.3 Hz, B/B′), 8.19 (d, 1H, J = 8.3 Hz, B/B′).

Cyclophane Pd(II) Carbonyl Complexes. All complexes were synthesized by the reported method.[20] As the spectral data for the BAF^- counterion were previously reported, only the characterization of the cations is given below.

[(NMe$_2$-Cyc)PdMe(CO)]$^+$ (15a). ^{1}H NMR (500 MHz, CD_2Cl_2) δ 1.02 (s, 3H), 2.90−3.18 (m, 8H), 3.00 (s, 6H), 6.28 (d, 2H, J = 7.9 Hz), 6.39 (d, 2H, J = 7.8 Hz), 6.52 (d, 2H, J = 7.9 Hz), 6.63 (s, 2H), 6.64 (s, 2H), 6.71 (d, 2H, J = 7.9 Hz), 6.87 (d, 1H, J = 7.2 Hz), 6.96 (d, 2H, J = 7.6 Hz), 7.03 (d, 2H, J = 7.7 Hz), 7.07 (d, 2H, J = 7.6 Hz), 7.10−7.15 (m, 3H), 7.69 (t, 2H, obscured by BAF^-), 8.17 (d, 1H, J = 8.3 Hz), 8.21 (d, 1H, J = 8.3 Hz); ^{13}C NMR (125 MHz, CD_2Cl_2) δ 10.5, 34.38, 34.58, 40.66, 40.73, 113.86, 113.88, 126.27, 126.46, 127.110, 127.66, 127.71, 127.95, 128.30, 128.51, 128.88, 129.64, 129.80, 129.86, 129.98, 130.19, 130.42, 131.9, 133.04, 134.06, 135.28, 135.86, 136.11, 136.16, 140.43, 140.45, 146.2, 149.94, 150.12, 173.8, 175.2, 180.1; IR (thin film) 2119.4 cm^{-1} [ν(CO)].

[(OMe-Cyc)PdMe(CO)]$^+$ (15b). ^{1}H NMR (500 MHz, CD_2Cl_2) δ 1.02 (s, 3H), 2.90−3.17 (m, 8H), 3.86 (s, 3H), 6.28 (d, 2H, J = 7.7 Hz), 6.39 (d, 2H, J = 7.9 Hz), 6.53 (d, 2H, J = 8.0 Hz), 6.73 (d, 2H, J = 7.9 Hz), 6.79 (d, 1H, J = 7.3 Hz), 6.92 (s, 2H), 6.94 (s, 2H), 6.96 (d, 2H, J = 7.9 Hz), 7.02 (d, 2H, J = 7.9 Hz), 7.07 (d, 2H, J = 7.9 Hz), 7.10 (d, 1H, J = 7.3 Hz), 7.14 (d, 2H, J = 7.9 Hz), 7.68 (t, 2H, obscured by BAF^-), 8.21 (d, 1H, J = 8.3 Hz), 8.24 (d, 1H, J = 8.3 Hz); ^{13}C NMR (125 MHz, CD_2Cl_2) δ 10.5, 34.45, 34.64, 56.3, 116.59, 116.78, 125.94, 126.66, 126.80, 127.56, 127.82, 127.87, 128.18, 128.35, 129.88, 130.00, 130.08, 130.16, 130.36, 130.59, 132.45, 133.56, 134.58, 134.78, 135.09, 136.00, 136.85, 137.33, 140.89, 140.93, 146.6, 159.19, 159.45, 173.6, 174.8, 179.8; IR (thin film) 2123.3 cm^{-1} [ν(CO)].

[(Me-Cyc)PdMe(CO)]$^+$ (15c). ^{1}H NMR (500 MHz, CD_2Cl_2) δ 1.01 (s, 3H), 2.46 (s, 3H), 2.47 (s, 3H), 2.87 − 3.20 (m, 8H), 6.27 (d, 2H, J = 7.7 Hz), 6.38 (d, 2H, J = 7.8 Hz), 6.52 (d, 2H, J = 7.8 Hz), 6.68−6.75 (m, 3H), 6.95 (d, 2H, J = 7.8 Hz), 7.00 (d, 2H, J = 7.8 Hz), 7.05 (d, 2H, J = 7.7 Hz), 7.14 (d, 2H, J = 7.9 Hz), 7.20−7.24 (m, 5H), 7.68 (t, 2H, obscured by BAF^-), 8.19 (d, 1H, J = 8.3 Hz), 8.23 (d, 1H, J = 8.3 Hz); ^{13}C NMR (125 MHz, CD_2Cl_2) δ 10.3, 21.28, 21.35, 34.51, 34.71, 125.92, 126.22, 126.69, 126.78, 127.65, 127.89, 128.25, 128.39, 128.45, 129.86, 129.98, 130.07, 130.12, 130.31, 130.57, 132.03, 132.26, 133.54, 134.43, 134.55, 134.87, 136.77, 139.01, 139.61, 140.74, 140.77, 141.56, 146.6, 172.9, 174.8, 179.2; IR (thin film) 2123.3 cm^{-1} [ν(CO)].

[(Cl-Cyc)PdMe(CO)]$^+$ (15d). ^{1}H NMR (500 MHz, CD_2Cl_2) δ 1.03 (s, 3H), 2.87−3.21 (m, 8H), 6.27 (d, 2H, J = 7.9 Hz), 6.41 (d, 2H, J = 7.8 Hz), 6.52 (d, 2H, J = 7.9 Hz), 6.75 (d, 2H, J = 7.8 Hz), 6.83 (d, 1H, J = 7.3 Hz), 6.97 (d, 2H, J = 7.7 Hz), 6.99−7.05 (m, 4H), 7.13−7.18 (m, 3H), 7.43 (s, 3H), 7.46 (s, 3H), 7.68−7.78 (m, 2H, partially obscured by BAF^-), 8.25 (d, 1H, J = 8.3 Hz), 8.28 (d, 1H, J = 8.2 Hz); ^{13}C NMR (125 MHz, CD_2Cl_2) δ 10.7, 34.46, 34.66, 125.55, 126.42, 126.88, 127.48, 127.74, 128.10, 128.18, 130.14, 130.25, 130.32, 130.43, 130.60, 130.79, 131.50, 131.71, 132.16, 133.40, 133.40, 133.73, 134.19, 134.26, 134.83, 135.21, 136.45, 137.27, 137.75, 141.45, 141.51, 142.36, 146.9, 173.03, 174.36, 179.4; IR (Thin film) 2127.1 cm^{-1} [ν(CO)].

[(CF$_3$-Cyc)PdMe(CO)]$^+$ (15e). ^{1}H NMR (500 MHz, CD_2Cl_2) δ 1.02 (s, 3H), 2.90−3.22 (m, 8H), 6.31 (d, 2H, J = 7.8 Hz), 6.44 (d, 2H, J = 7.8 Hz), 6.56 (d, 2H, J = 7.7 Hz), 6.74 (d, 1H, J = 7.3 Hz), 6.79 (d, 2H, J = 8.0 Hz), 6.99 (d, 2H, J = 7.8 Hz), 7.01−7.08 (m, 5H), 7.19 (d, 2H, J = 7.9 Hz), 7.68−7.78 (m, 6H, partially obscured by BAF^-), 8.26 (d, 1H, J = 8.3 Hz), 8.30 (d, 1H, J = 8.3 Hz); ^{13}C NMR (125 MHz, CD_2Cl_2) δ 10.9, 34.46, 34.66, 123.88 (q, $^1J_{CF}$ = 273.3 Hz), 123.94 (q, $^1J_{CF}$ = 273.3 Hz), 125.4, 126.24, 126.89, 127.51, 127.78, 128.15, 128.79 (q, $^2J_{CF}$ = 24.0 Hz), 130.29, 130.39, 130.46, 130.60, 130.73, 130.91, 132.23, 133.21, 133.53, 134.51, 135.53, 135.91, 136.79, 141.71, 141.78, 141.96, 146.39, 147.11, 172.6, 174.1, 179.0; IR (thin film) 2127.1 cm^{-1} [ν(CO)].

General Procedure for Ni(II)-Catalyzed Polymerizations. A 600 mL autoclave was heated under vacuum to 120 °C for 2 h, then twice purged with ethylene, and adjusted to the desired polymerization temperature by external oil bath. A flask was charged with a desired amount of Ni(II) catalyst under a nitrogen atmosphere, and to this was added 10 mL of 1,2-dichlorobenzene. In a separate flask was added 80 mL of dry toluene or 1,2-dichlorobenzene, the latter solvent if the polymerization was conducted at temperatures higher than 80 °C, and a suitable amount of aluminum coactivator solution in toluene ([Al]/[Ni] = 1500). An additional 10 mL of solvent was set aside. The solution of Al activator was then transferred into the reactor by vacuum under a nitrogen stream. Ethylene was introduced to a pressure of 200 psi, and the mixture was rapidly stirred for 10 min and then vented. The catalyst solution was transferred into the reactor by vacuum under a nitrogen stream and flushed with the final 10 mL of solvent. The reactor was filled with ethylene to 200 psi, and the polymerization was allowed to proceed for the desired time with rapid stirring. The reactor was vented, a mixture of 70 mL of acetone, 30 mL of methanol, and 1 mL of concentrated hydrochloric acid was transferred into the reactor by vacuum, the autoclave was opened, and the polymer was collected, decanted, and dried *in vacuo* at 80 °C overnight. The reactor was twice cleaned with boiling toluene before subsequent polymerizations.

Aluminum Coactivator Screen. The general procedure for Ni(II)-catalyzed polymerizations was followed using 1.0 μmol of catalyst and 1500 equiv of the coactivator of choice. Polymerizations were run for 10 min at 35 or 80 °C.

Variable-Temperature Screen. The general procedure for Ni-(II)-catalyzed polymerizations was followed using 1.0 μmol of catalyst and triisobutylaluminum as the coactivator (1.5 mL of a 10% w/w solution in toluene, 1.0 M). Polymerizations were run for 10 min at the desired temperature.

Thermal Stability Study at 80 °C. The general procedure for Ni(II)-catalyzed polymerizations was followed using 0.5 μmol of catalysts and triisobutylaluminum as the coactivator (1.5 mL of a 10% w/w solution in toluene, 1.0 M). Temperature was maintained at 80 °C.

General Procedure for Pd(II)-Catalyzed Ethylene Homopolymerizations. An oven-dried two-neck flask was charged with 20 μmol of Pd(II) catalyst and 30 μmol of NaBAF under a nitrogen atmosphere, and to this was added 50 mL of dry toluene. In the case for polymerizations run at elevated temperature, a reflux condenser was attached. Temperature was controlled by placement in an external bath as needed. For the duration of the polymerization, ethylene was slowly bubbled through the solution with stirring to maintain ambient pressure. At 3, 6, and 20 h, 10 mL aliquots of the polymerization mixture were removed and the solvent was dried *in vacuo* to afford the polymer. To compensate for solvent evaporation and/or polymer formation, the volume of remaining reaction mixture was measured immediately after the removal of each aliquot by syringe. After 48 h, the flow of ethylene

was stopped and the polymerization mixture was concentrated *in vacuo* to afford the final yield of polymer.

General Procedure for Methyl Acrylate−Ethylene Copolymerization. A 250 mL oven-dried autoclave was charged with 10 μmol of Pd(II) complex and 15 μmol of NaBAF, if necessary, under a nitrogen atmosphere. Dry toluene was added, followed by a known amount of methyl acrylate, so that the solution volume was 50 mL with the desired acrylate concentration. To promote catalyst solubility, 15 mL of toluene may be substituted with chlorobenzene. The autoclave was closed, 88 psi of ethylene was introduced, and the mixture was stirred for 18 h at room temperature. The reactor was vented, and the mixture concentrated *in vacuo* and then dried for 24 h under vacuum at 70 °C.

SEC Characterization of Polymers. All polymers were characterized by size-exclusion chromatography (SEC). All polymers produced by the Pd(II) catalysts were soluble in THF and were eluted through a 30 cm size-exclusion column (Polymer Laboratories PLgel Mixed C, 5 μm particle size) to separate polymer samples. Measurements were made on highly dilute fractions eluting from a SEC consisting of a HP Aglient 1100 solvent delivery system/auto injector with an online solvent degasser, a temperature-controlled column compartment, and an Aglient 1100 differential refractometer. The mobile phase was THF, and the flow rate was 1.0 mL/min. A Dawn DSP 18-angle multiangle light scattering (MALS) detector (Wyatt Technology, Santa Barbara, CA) was coupled to the SEC to measure both the MW and sizes for each fraction of the polymer eluted from the SEC column.[29,46] Both the column and the differential refractometer were held at 35 °C. A 30 μL sample of a 2 mg/mL solution was injected into the column. ASTRA 4.7 from Wyatt Technology was used to acquire data from the 18 scattering angles (detectors) and the differential refractometer. The M_n and M_w data were obtained by following classical light-scattering treatments. Polymers prepared by the Ni(II) catalysts were insufficiently soluble in THF and were instead analyzed by SEC in 1,2,4-trichlorobenzene at 140 °C by the Polymer Characterization Facility at the Cornell Center for Materials Research, Cornell University, Ithaca, NY. The M_n and M_w data were obtained by comparison to a polyethylene or polystyrene standard at the Cornell and UCSB facilities, respectively.

NMR Analysis of Polymers. Branching densities *B* were calculated by the ratio of methyl group integration to total hydrocarbon integration using ^{1}H NMR. Samples of polymer prepared by the Ni(II) catalysts were dissolved in hot 1,1,2,2-tetrachloroethane-d_2, and spectra were acquired at 140 °C. Samples of polymers from the Pd(II) catalysts were dissolved in $CDCl_3$ and acquired at 25 °C.

■ ASSOCIATED CONTENT

Supporting Information. A figure showing polymerization productivity of Ni(II) catalysts with different Al activators, a plot of chemical shift versus substituent for the Pd-Me resonance, and 2D NMR and NOE data for complexes **3c**, **18**, and **19**. This material is available free of charge via the Internet at http://pubs.acs.org.

■ AUTHOR INFORMATION

Corresponding Author
*E-mail: zguan@uci.edu.

■ ACKNOWLEDGMENT

We thank the National Science Foundation (Chem-0456719, Chem-0723497, DMR-0703988) for funding. C.S.P. acknowledges the Allergan Foundation, the UCI Department of Chemistry, and Joan Rowland for financial support. C.M.L. acknowledges a SURF-IT undergraduate research fellowship. Z.G. acknowledges a Camille Dreyfus Teacher-Scholar Award.

■ REFERENCES

(1) This paper has been adapted in part from the following thesis: Popeney, C. S. Ph.D. Dissertation, University of California at Irvine, 2008.
(2) Moehring, V. M.; Fink, G. *Angew. Chem., Int. Ed. Engl.* **1985**, *24*, 1001–1003.
(3) Johnson, L. K.; Killian, C. M.; Brookhart, M. *J. Am. Chem. Soc.* **1995**, *117*, 6414–6415.
(4) Ittel, S. D.; Johnson, L. K.; Brookhart, M. *Chem. Rev.* **2000**, *100*, 1169–1203.
(5) Johnson, L. K.; Mecking, S.; Brookhart, M. *J. Am. Chem. Soc.* **1996**, *118*, 267–268.
(6) Held, A.; Bauers, F. M.; Mecking, S. *Chem. Commun.* **2000**, 301–302.
(7) Mecking, S.; Johnson, L. K.; Wang, L.; Brookhart, M. *J. Am. Chem. Soc.* **1998**, *120*, 888–899.
(8) Chen, G.; Ma, X. S.; Guan, Z. *J. Am. Chem. Soc.* **2003**, *125*, 6697–6704.
(9) Gates, D. P.; Svejda, S. K.; Onate, E.; Killian, C. M.; Johnson, L. K.; White, P. S.; Brookhart, M. *Macromolecules* **2000**, *33*, 2320–2334.
(10) Tempel, D. J.; Johnson, L. K.; Huff, R. L.; White, P. S.; Brookhart, M. *J. Am. Chem. Soc.* **2000**, *122*, 6686–6700.
(11) Xie, T.; McAuley, K. B.; Hsu, J. C. C.; Bacon, D. W. *Ind. Eng. Chem. Res.* **1994**, *33*, 449–479.
(12) Camacho, D. H.; Salo, E. V.; Ziller, J. W.; Guan, Z. *Angew. Chem., Int. Ed.* **2004**, *43*, 1821–1825.
(13) Camacho, D. H.; Salo, E. V.; Guan, Z. *Org. Lett.* **2004**, *6*, 865–868.
(14) Camacho, D. H.; Guan, Z. *Macromolecules* **2005**, *38*, 2544–2546.
(15) Chen, C.-T.; Gantzel, P.; Siegel, J. S.; Baldridge, K. K.; English, R. B.; Ho, D. M. *Angew. Chem., Int. Ed. Engl.* **1995**, *34*, 2657–2660.
(16) Cram, D. J. *Angew. Chem., Int. Ed. Engl.* **1986**, *25*, 1039–1057.
(17) Chiu, S.-H.; Stoddart, J. F. *J. Am. Chem. Soc.* **2002**, *124*, 4174–4175.
(18) Popeney, C. S.; Camacho, D. H.; Guan, Z. *J. Am. Chem. Soc.* **2007**, *129*, 10062–10063.
(19) Popeney, C. S.; Guan, Z. *J. Am. Chem. Soc.* **2009**, *131*, 12384–12393.
(20) Popeney, C.; Guan, Z. *Organometallics* **2005**, *24*, 1145–1155.
(21) Popeney, C. S.; Guan, Z. *Macromolecules* **2010**, *43*, 4091–4097.
(22) Kajigaeshi, S.; Kakinami, T.; Inoue, K.; Kondo, M.; Nakamura, H.; Fujikawa, M.; Okamoto, T. *Bull. Chem. Soc. Jpn.* **1988**, *61*, 597–599.
(23) Barder, T. E.; Walker, S. D.; Martinelli, J. R.; Buchwald, S. L. *J. Am. Chem. Soc.* **2005**, *127*, 4685–4696.
(24) Moody, L. S.; Mackenzie, P. B.; Killian, C. M.; Lavoie, G. G.; Ponasik, J. A., Jr.; Barrett, A. G.; Smith, T. W.; Pearson, J. C. WO 00/50470, 2002.
(25) Meinhard, D.; Wegner, M.; Kipiani, G.; Hearley, A.; Reuter, P.; Fischer, S.; Marti, O.; Rieger, B. *J. Am. Chem. Soc.* **2007**, *129*, 9182–9191.
(26) Popeney, C. S.; Rheingold, A. L.; Guan, Z. *Organometallics* **2009**, *28*, 4452–4463.
(27) Salo, E. V.; Guan, Z. *Organometallics* **2003**, *22*, 5033–5046.
(28) Hansch, C.; Leo, A.; Taft, R. W. *Chem. Rev.* **1991**, *91*, 165–195.
(29) Guan, Z.; Cotts, P. M.; McCord, E. F.; McLain, S. J. *Science* **1999**, *283*, 2059–2062.
(30) Xie, T.; Penelle, J.; Verraver, M. *Polymer* **2002**, *43*, 3973–3977.
(31) Schmid, M.; Eberhardt, R.; Klinga, M.; Leskela, M.; Rieger, B. *Organometallics* **2001**, *20*, 2321–2330.
(32) Wadepohl, H.; Kohl, U.; Bittner, M.; Koppel, H. *Organometallics* **2005**, *24*, 2097–2105.
(33) Leatherman, M.; Svejda, S. A.; Johnson, L. K.; Brookhart, M. *J. Am. Chem. Soc.* **2003**, *125*, 3068–3081.
(34) Crabtree, R. H. *The Organometallic Chemistry of the Transition Metals*, 3rd ed.; John Wiley and Sons, Inc: New York, 2001.
(35) Halpern, J. *Inorg. Chim. Acta* **1985**, *100*, 41–48.

(36) Jones, W. D.; Feher, F. J. *J. Am. Chem. Soc.* **1986**, *108*, 4814–4819.
(37) Shultz, L. H.; Tempel, D. J.; Brookhart, M. *J. Am. Chem. Soc.* **2001**, *123*, 11539–11555.
(38) Plutino, M. R.; Scolaro, L. M.; Romeo, R.; Grassi, A. *Inorg. Chem.* **2000**, *39*, 2712–2720.
(39) Marrone, A.; Re, N.; Romeo, R. *Organometallics* **2008**, *27*, 2215–2222.
(40) Woo, T. K.; Blochl, P. E.; Ziegler, T. *J. Phys. Chem. A* **2000**, *104*, 121–129.
(41) Lee, L.-s.; Ou, H.-j.; Hsu, H.-l. *Fluid Phase Equilib.* **2005**, *231*, 221–230.
(42) Pangborn, A. B.; Giardello, M. A.; Grubbs, R. H.; Rosen, R. K.; Timmers, F. J. *Organometallics* **1996**, *15*, 1518–1520.
(43) Yakelis, N. A.; Bergman, R. G. *Organometallics* **2005**, *24*, 3579–3581.
(44) Dale, W. J.; Rush, J. E. *J. Org. Chem.* **1962**, *27*, 2598–2603.
(45) Vanasselt, R.; Gielens, E. E. C. G.; Rulke, R. E.; Vrieze, K.; Elsevier, C. J. *J. Am. Chem. Soc.* **1994**, *116*, 977–985.
(46) Cotts, P. M.; Guan, Z.; McCord, E.; McLain, S. *Macromolecules* **2000**, *33*, 6945–6952.